Second International Conference on
Geometry, Integrability and Quantization
June 7–15, 2000, Varna, Bulgaria
Ivaïlo M. Mladenov and Gregory L. Naber, Editors
**Coral Press**, Sofia 2001

# QUANTUM HOLOGRAM AND RELATIVISTIC HODOGRAM: MAGNETIC RESONANCE TOMOGRAPHY AND GRAVITATIONAL WAVELET DETECTION

ERNST BINZ[†] and WALTER SCHEMPP[‡]

[†] *Lehrstuhl für Mathematik I, Universität Mannheim, D-68159 Mannheim, Germany*
[‡] *Lehrstuhl für Mathematik I, Universität Siegen, D-57068 Siegen, Germany*

**Abstract**. Quantum holography is a well established theory of mathematical physics based on harmonic analysis on the Heisenberg Lie group $G$. The geometric quantization is performed by projectivization of the complexified coadjoint orbit picture of the unitary dual $\hat{G}$ of $G$ in order to achieve a geometric adjustment of the quantum scenario to special relativity theory. It admits applications to various imaging modalities such as synthetic aperture radar (SAR) in the microwave range, and, most importantly for the field of non-invasive medical diagnosis, to the clinical imaging modality of magnetic resonance tomography (MRI) in the radiofrequency range. Quantum holography explains the quantum teleportation phenomenon through Einstein–Podolsky–Rosen (EPR) channels which is a consequence of the non-locality of phase coherent quantum field theory, the concept of absolute simultaneity of special relativity theory which provides the Einstein equivalence of energy and Fitzgerald–Lorentz dilated mass, and the perfect holographic replication process of molecular genetics. It specifically reveals what was before unobservable in quantum optics, namely the interference phenomena of matter wavelets of Bose–Einstein condensates, and what was before unobservable in special relativity, namely the light in flight (LIF) recording processing by ultrafast laser pulse trains. Finally, it provides a Lie group theoretical approach to the Kruskal coordinatized Schwarzschild manifold of quantum cosmology with large scale applications to general relativity theory such as gravitational instanton symmetries and the theory of black holes. The direct spinorial detection of gravitational wavelets emitted by the binary radio pulsar PSR 1913+16 and known only indirectly so far will also be based on the principles of quantum holography applied to very large array (VLA) radio interferometers.

## 1. Introduction

All mathematical descriptions of quantum fields are inherently based on dynamical symmetries in a wide geometric sense [19,49]. Similarly, in general relativity theory exact solutions of the Einstein field equations cannot be found except in spacetime manifolds admitting a high degree of symmetry. Quantum holography is based on the projectivization $\mathbb{CP}^2$ under its standard Kähler metric of the complexification of the symplectic affine plane $\mathbb{R} \oplus \mathbb{R}$. Recall that a **Kähler manifold** is a complex manifold which is equipped with a Hermitian metric on its holomorphic tangent bundle, whose imaginary part is a closed exterior differential (1,1)-form, and which thus defines a symplectic structure on the complex manifold itself. The standard construction of complex projective plane

$$\mathbb{CP}^2 = \left(\mathbb{C}^3 - \{0\}\right)/\mathbb{C}^\times$$

provides the prototype of a two-dimensional compact Kähler manifold which is a compact Hodge manifold [65]. Because its standard symplectic structure follows in a natural way from any *planar* coadjoint orbit $\mathcal{O}$ of the unitary dual $\hat{G}$ of the Heisenberg nilpotent Lie group $G$ [54], the following statement by the Nobel prize winner Abdus Salam on the importance of group theory in physics is highly relevant for the appreciation of the Lie group representational approach [52] to phase coherent optics and microwave radar imaging, quantum optics of Bose–Einstein condensates, relativistic astrophysics of gravitational wavelets, molecular genetic information processing, clinical MRI, quantum information theory, and phase coherent quantum field theory.

> *Throughout the history of quantum theory, a battle has raged between the amateurs and professional group theorists. The amateurs have maintained that everything one needs in the theory of groups can be discovered by the light of nature provided one knows how to multiply two matrices. In support of this claim, they of course, justiably, point to the successes of that prince of amateurs in this field, Dirac, particularly with the spinor representations of the Lorentz group. As an amateur myself, I strongly believe in the truth of the non-professional creed. I think perhaps there is not much one has to learn in the way of methodology from the group theorists except caution. But this does not mean one should not be aware of the riches which have been amassed over the course of years particularly in the most highly developed of all mathematical disciplines — the theory of Lie groups. My lectures then are an amateur's attempt to gather some of the fascinating results for compact simple Lie groups which are likely to be of physical interest. I shall state theorems; and with a physicist's*

*typical unconcern rarely, if ever, shall I prove them. Throughout, the emphasis will be to show the close similarity of these general groups with the most familiar of all groups, the group of rotations in three dimensions. In 1951 I had the good fortune to listen to Professor Racah lecture on Lie group at Princeton. After attending these lectures I thought this is really too hard; I cannot learn this; one is hardly ever likely to need all this complicated matter. I was completely wrong. Eleven years later the wheel has gone full cycle and it is my turn to lecture on this subject. I am sure many of you will feel after these lectures that all this is too damned hard and unphysical. The only thing I can say is: I do very much hope and wish you do not have to learn this beautiful theory eleven years too late.*

In the Heisenberg group geometric quantization procedure, the role of the spinor representation will be played by the metaplectic representation $\omega$ of the metaplectic group $Mp(2,\mathbb{R})$ which leaves fixed the points $\nu \neq 0$ along the longitudinal direction of the one-dimensional *timelike* center $C \hookrightarrow G$ [66]. In the associated center-time splitting, the complexification of $C$ is embedded into the complex projective plane $\mathbb{CP}^2$ which permits to attach to each planar coadjoint orbit

$$\mathcal{O} = \mathcal{O}_\nu\,, \qquad \nu \in \mathbb{R}^\times$$

the negatively curved *eigen* time shell of the Milne explosion cosmos of global expansion parameter $\nu$. Each eigen time shell is located within the light cone of the Minkowskian spacetime manifold.

In the relativistic hodogram associated to the quantum hologram via the eigen time shell, the non-linear Einstein composition of *global* radial velocities

$$(v_1, v_2) \rightsquigarrow \frac{v_1 + v_2}{1 + v_1 v_2}$$

corresponds to the chain rule of cross-ratios in $\mathbb{CP}^2$. Specifically, the composition law applied to any radial velocity $v_1 = v$, $|v| < 1$, and the velocity of light $v_2 = 1$ preserves the limiting velocity of light $v_2 = 1$. The group of Lorentz transformations is then considered as a Lie group of *rotational* collineations of the complex projective plane $\mathbb{CP}^2$ which acts on the *conformally* invariant two-dimensional sphere

$$\sqrt{2\pi|\nu|}\,.\,\mathbb{S}^2 \hookrightarrow \mathbb{CP}^2\,, \qquad \nu \neq 0$$

of the sandwich *trace* configuration of mirrored pairs of planar coadjoint orbits

$$(\mathcal{O}_\nu, \mathcal{O}_{-\nu})\,, \qquad \nu \in \mathbb{R}^\times\,.$$

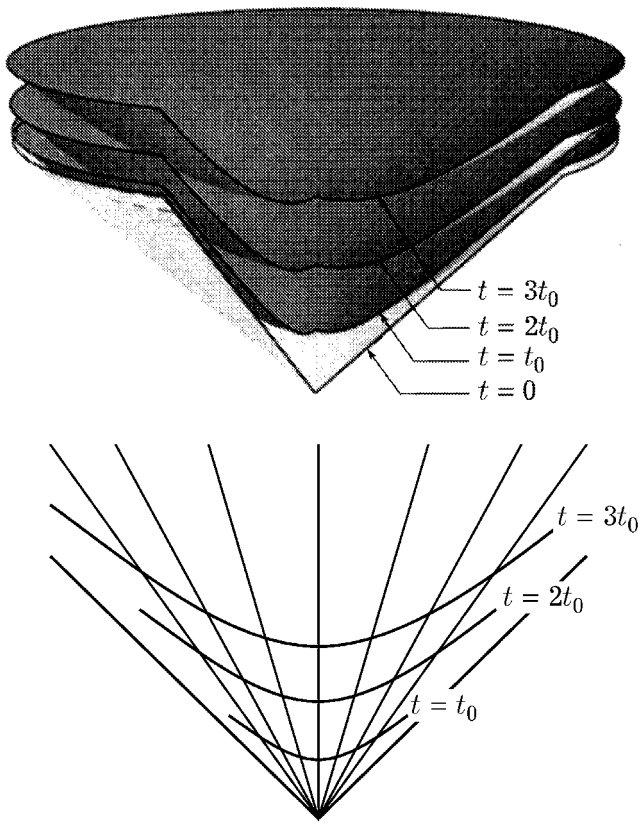


**Figure 1.** The Milne cosmos displaying three stages of an expanding curved space The transversal sections of the negatively curved eigen time shells within the light cone $t = 0$ are circular and reflect the natural symplectic structure of the planar coadjoint orbits $\mathcal{O}_\nu$ $(\nu \neq 0)$ of the Heisenberg nilpotent Lie group $G$. Note that the symplectic structure gives rise to the orthogonality involution of conjugate lines in the complex projective metric plane $\mathbb{CP}^2$, and therefore to the four focal points of the elliptic, hyperbolic and the single focus of the parabolic motions, the focal points being the intersections of the isotropic tangents to the one-dimensional central projective quadric. The two real or imaginary foci determine the other two, as the non-cyclic intersection points of the isotropic lines going through the given foci. Both pairs are symmetric with respect to the center. Similarly, the focus of a parabola lies on its axis. The planar section through the Milne cosmos reveals the same isotropic lines as in the Minkowski world. The world trajectories form a pencil of timelike lines.

The Lorentz group implements a timelike orthogonality involution corresponding to the natural involution of

$$\log_{\mathfrak{g}} C \hookrightarrow \mathfrak{g}$$

under the logarithmic scale of the real **Heisenberg Lie algebra**. The logarithmic scale is compatible with the Kähler metric of the compact complex manifold $\mathbb{CP}^2$ [65]. The associated center-time splitting induces projectively

as Möbius transformations the Lorentz transformations of symmetric matrix

$$\begin{pmatrix} \dfrac{1}{\sqrt{1-v^2}} & -\dfrac{v}{\sqrt{1-v^2}} \\ -\dfrac{v}{\sqrt{1-v^2}} & \dfrac{1}{\sqrt{1-v^2}} \end{pmatrix} .$$

The Lorentz matrix is written in natural units where the speed of light is one and $v$ denotes a real number such that $|v| < 1$. Scaling the global radial velocity $v$ to the velocity of light $c$ yields the real matrix

$$\begin{pmatrix} \dfrac{1}{\sqrt{1-v^2/c^2}} & -\dfrac{v}{\sqrt{1-v^2/c^2}} \\ -\dfrac{v}{c^2\sqrt{1-v^2/c^2}} & \dfrac{1}{\sqrt{1-v^2/c^2}} \end{pmatrix} , \qquad |v| < c .$$

Due to the factor $1/c^2$, the *scaled* matrix lacks the property of symmetry for $v \neq 0$. Under the logarithmic scale on the one-dimensional timelike center $C \hookrightarrow G$, the symmetry of the orthogonality involution will be restored by the Einstein equivalence of energy $\mathcal{E}$ and Fitzgerald–Lorentz dilated mass

$$m = \frac{m_0}{\sqrt{1-v^2/c^2}} , \qquad |v| < c ,$$

where $m_0$ denotes the rest mass (see below).

Due to the fact that every first order *cocycle* of every non-trivial element of the unitary dual $\hat{G}$ forms a *coboundary*, the Lorentz group respects the Stone–von Neumann theorem of quantum physics [46, 54], hence the sandwich trace configuration of mirrored pairs of planar coadjoint orbits $(\mathcal{O}_\nu, \mathcal{O}_{-\nu})$, or the Hopf fibration to be discussed below. Up to reflections, the Lorentz transformations actually are the *only* rotational collineations of $\mathbb{CP}^2$ which respect the isotropic lines, the phase angles, and the Stone–von Neumann theorem. This can be seen from the asymptotic cone of the dilated two-dimensional sphere

$$\sqrt{2\pi|\nu|} \, . \, \mathbb{S}^2 \hookrightarrow \mathbb{CP}^2 , \qquad \nu \neq 0$$

which isotropically *linearizes* this conformally invariant two-dimensional sphere of $\mathbb{R}^3$ as well as the half-density associated to the logarithmic scale. It follows that the compatibility with quantum physics nicely *characterizes* the group of Lorentz transformations of special relativity theory and the reflections as the group of automorphisms of the sandwich trace configuration. Therefore, the *metaphor* of the sandwich trace configuration as a visualization "more geometrico" of the group representational *induction* process forms a system draft

(Entwurf) in the sense of Immanuel Kant's critique of the pure reason visualizing the epistemologic *horizon* of human knowledge and its immanent system *conceptions*.

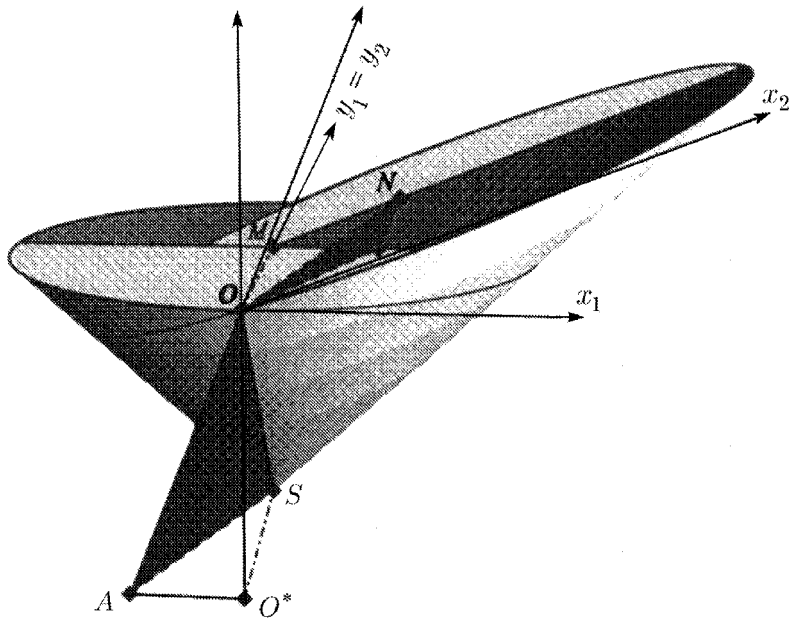


**Figure 2.** Visualization of the shear associated to a Lorentz transformation and the relativistic Doppler filter bank effect of multirate signal analysis or subband coding. In contrast to the group of Galilean transformations, the group of Lorentz transformations respects the Stone–von Neumann theorem of quantum physics as the group of rotational collineations of the complex projective plane $\mathbb{CP}^2$. The center-time splitting yields the Einstein equivalence of energy $\mathcal{E}$ and Fitzgerald–Lorentz dilated mass $m$ by means of the Third Keplerian Law of planetary motion, and the relativistic Doppler filter bank effect.

Projectivization of the planar coadjoint orbits $(\mathcal{O}_\nu, \mathcal{O}_{-\nu})$ and affine deprojectivization of the conformally invariant sphere $\sqrt{2\pi|\nu|}\,.\,\mathbb{S}^2$ provides the Dandelin–Quételet construction of the First Keplerian Law of planetary motion. In contrast to the group of Lorentz transformations, the Galilean group violates the symmetries of the sandwich trace configuration because it relates the one-dimensional timelike center $C \hookrightarrow G$ to the time $t \in \mathbb{R}$ but conversely *not* the time axis $\mathbb{R}$ to $C$. Due to the missing timelike orthogonality involution of the center-time splitting, the group of Galilean transformations of velocity matrix

$$\begin{pmatrix} 1 & -v \\ 0 & 1 \end{pmatrix}$$

does no respect the Stone–von Neumann theorem as a limiting case of the group of Lorentz transformations nor does it provide the Einstein equivalence of

energy $\mathcal{E}$ and Fitzgerald–Lorentz dilated mass $m$. The Galilean transformations conflict with Maxwell's laws of electrodynamics as well as quantum mechanics. The cocompact lattice $\mathbb{Z}^3 \hookrightarrow G$ suggests to conceive $G$ as a principal circle bundle over the two-dimensional compact torus $\mathbb{T}^2 = \mathbb{R}^2/\mathbb{Z}^2$. The compact nilmanifold $G/\mathbb{Z}^3$ suggest to conceive $\mathbb{CP}^2$ as a complex projective (hyper-) plane of the compact Kähler manifold of circles $\mathbb{CP}^3$. Then each complex projective line of the *linear* manifold of circles $\mathbb{CP}^2$ forms a pencil of circles.

## 2. The Real Heisenberg Lie Group and Lie Algebra

A central role in the study of the cotangent bundle $\mathrm{T}^\star\mathbb{R}^2$ is played by the real **Heisenberg Lie group** $G$. The three-dimensional connected and simply connected Heisenberg nilpotent Lie group $G$ forms the non-split *central* group extension

$$\mathbb{R} \lhd G \longrightarrow \mathbb{R} \oplus \mathbb{R}\,.$$

The concept of central extension is of fundamental importance in the theory of loop groups.

The standard presentation of $G$ is given by the multiplication law $(g_1, g_2) \rightsquigarrow g_1 g_2$ of unipotent matrices with real entries

$$\begin{pmatrix} 1 & x_1 & z_1 \\ 0 & 1 & y_1 \\ 0 & 0 & 1 \end{pmatrix} \begin{pmatrix} 1 & x_2 & z_2 \\ 0 & 1 & y_2 \\ 0 & 0 & 1 \end{pmatrix} = \begin{pmatrix} 1 & x_1 + x_2 & z_1 + z_2 + x_1 y_2 \\ 0 & 1 & y_1 + y_2 \\ 0 & 0 & 1 \end{pmatrix}.$$

All the eigenvalues of the elements $g \in G$ are equal to 1, the neutral element of $G$ is given by the unit matrix

$$\begin{pmatrix} 1 & 0 & 0 \\ 0 & 1 & 0 \\ 0 & 0 & 1 \end{pmatrix},$$

and the inverse $g^{-1} \in G$ obviously reads

$$\begin{pmatrix} 1 & x & z \\ 0 & 1 & y \\ 0 & 0 & 1 \end{pmatrix}^{-1} = \begin{pmatrix} 1 & -x & -z + xy \\ 0 & 1 & -y \\ 0 & 0 & 1 \end{pmatrix}.$$

The point to note is that, in the standard presentation, $G$ forms a linear superposition of *transvections* which allow a geometric adjustment of the world lines or photon trajectories of the experimental setup to the convex light cone [32]. Due the transvectional interpretation of the elements of $G$, the geometry of the Heisenberg nilpotent Lie group $G$ is *compatible* with the rotational collineations of $\mathbb{CP}^2$ forming the Lorentz group.

Using ultrafast laser pulse trains, the compatibility of quantum holography with special relativity theory has been experimentally confirmed by LIF recording processing [1–5, 64]. In relativistic astrophysics, the indirect spinorial detection of gravitational wavelets emitted by the "visible" 59-ms radio *pulsar* of the binary neutron star system PSR 1913+16 [35] represents another important proof of the compatibility of quantum holography with relativity theory at large scales [41].

Allied to the simply connected Lie group $G$ is the **three-dimensional real Heisenberg Lie algebra** $\mathfrak{g}$ of nilpotent matrices

$$\begin{pmatrix} 0 & a & c \\ 0 & 0 & b \\ 0 & 0 & 0 \end{pmatrix}, \qquad a, b, c \in \mathbb{R}.$$

In terms of the Lie bracket of $\mathfrak{g}$, the commutator of the canonical basis of $\mathfrak{g}$ allows to formulate the Heisenberg uncertainty principle as a *duality* equation

$$\left[ \begin{pmatrix} 0 & 1 & 0 \\ 0 & 0 & 0 \\ 0 & 0 & 0 \end{pmatrix}, \begin{pmatrix} 0 & 0 & 0 \\ 0 & 0 & 1 \\ 0 & 0 & 0 \end{pmatrix} \right] = \begin{pmatrix} 0 & 0 & 1 \\ 0 & 0 & 0 \\ 0 & 0 & 0 \end{pmatrix}.$$

Connecting $\mathfrak{g}$ and $G$ there is the exponential map

$$\exp_G : \mathfrak{g} \longrightarrow G$$

which forms a global diffeomorphism such that the identity

$$\exp_G \left( \begin{pmatrix} 0 & a & c \\ 0 & 0 & b \\ 0 & 0 & 0 \end{pmatrix} \right) = \begin{pmatrix} 1 & a & c + \frac{1}{2}ab \\ 0 & 1 & b \\ 0 & 0 & 1 \end{pmatrix}$$

holds. The adjoint action of $G$ on the **Heisenberg Lie algebra** $\mathfrak{g}$ is defined by the adjoint representation

$$\mathrm{Ad}_G : G \longrightarrow GL(\mathfrak{g})$$

so that the adjoint orbits of $G$ are formed by the bundle of lines parallel to the one-dimensional center but *different* from the center of $\mathfrak{g}$. Notice that the generic adjoint orbits are one-dimensional and therefore cannot be symplectic manifolds. By duality they can be represented as *singletons*.

The contragredient representation to the adjoint representation

$$\mathrm{Ad}^*_G : G \longrightarrow GL(\mathfrak{g}^\star)$$

gives rise to the coadjoint action of $G$ on the vector space dual $\mathfrak{g}^\star$ of the **real Heisenberg Lie algebra**. Thus, the adjoint and coadjoint actions are *not* isomorphic, and in particular there exists *no* invariant non-degenerate symmetric bilinear form on the three-dimensional real vector space $\mathfrak{g}$.

The cotangent bundle $\mathrm{T}^\star G$ of $G$ admits the representation

$$\mathrm{T}^\star G = G \times \mathfrak{g}^\star .$$

For any element $g \in G$ and linear form $\nu \in \mathfrak{c}^\star$ ($\mathfrak{c}$ is the Lie algebra of $C$), the element $\mathrm{Ad}^*_G(g)(\nu) \in \mathfrak{g}^\star$ is determined by the rule

$$\mathrm{Ad}^*_G(g)(\nu)(X) = \nu\left(\mathrm{Ad}_G(g^{-1})(X)\right)$$

for all vector fields $X \in \mathfrak{g}$. Thus the coordinate form $\nu \in \mathfrak{c}^\star$ generates the invariants and the Casimir functions which are constant on the coadjoint orbits or invariant under the coadjoint action $\mathrm{Ad}^*_G$.

## 3. Geometric Quantization

Research into Lie group representation theory is motivated by the dynamical symmetries inherent to the geometry of basic physical principles. A major source of the unity of Lie group representation theory is the philosophy of the coadjoint orbit method also known by the more fashionable term geometric quantization. It has been observed, however, as a technical point that the coadjoint orbit method is almost exclusively a method of interpretation, a way of *organizing* information on Lie group representation theory into a *coherent* pattern. It has been emphasized that the overall coherence of the coadjoint orbit technique provides little in the way of technical tools for proofs or explicit computations. Thus, for example, several of the major results of Harish–Chandra on unitary linear representations of semisimple Lie groups have found elegant interpretations in terms of the coadjoint orbit method. These interpretations have actually provided *no* shortcuts to Harish–Chandra's proofs of the representational results [34]. However, this angle of mathematical view is not wide enough, and too technical. It is exactly the capability of efficiently organizing quantum information which makes the complexified and then productively completed coadjoint orbit picture of the Heisenberg nilpotent Lie group $G$ such a valuable tool of constructing appropriate substrates or hypostases for quantum holography, as well as the *semantic* interpretation of the coherently recorded amount of quantum information. Therefore Salam's impressing appeal to learn Lie group theory for physical applications as soon as possible [52] should include the challenge to get acquainted with the simple and actually *not* "unphysical" aspects of the coadjoint orbit method in order to classify the isomorphy classes of irreducible unitary linear representations for a wide category of Lie groups.

Because the *phenomenon* of time occurs only in the representations of the real Heisenberg nilpotent Lie group $G$ as the points $\nu \neq 0$ on the real dual $\mathfrak{c}^\star$ of the Lie algebra of the one-dimensional timelike center $C \hookrightarrow G$ and the

real time axis of the complex representation space, it is important to classify the isomorphy classes of irreducible unitary linear representations of $G$. The classification of the unitary dual $\hat{G}$ follows from the coadjoint orbit picture of $G$ in the vector space dual of the real **Heisenberg Lie algebra** $\mathfrak{g}^\star$. Explicitly,

$$\mathrm{Ad}^*_G \begin{pmatrix} 1 & x & z \\ 0 & 1 & y \\ 0 & 0 & 1 \end{pmatrix} = \begin{pmatrix} 1 & 0 & -x \\ 0 & 1 & y \\ 0 & 0 & 1 \end{pmatrix} .$$

Identify the linear forms $\nu \in \mathfrak{g}^\star$ $(\nu \neq 0)$ with their central control gradient drifts. Due to the Pfaffian linear form $\mathrm{Pf}(.) \in \mathfrak{c}^\star$ which defines the Plancherel measure $2|\nu|\,\mathrm{d}\nu$ on the timelike center $C \hookrightarrow G$, the natural symplectic forms

$$\lambda_{\mathcal{O}_\nu} = \nu\,.\,\mathrm{d}x \wedge \mathrm{d}y$$

associated with the oriented planar coadjoint orbits

$$\mathcal{O}_\nu = \mathrm{Ad}^*_G(G)(\nu)\,, \qquad \nu \in \mathbb{R}^\times$$

of $G$ exhibit the real variable $x$ as a local spatial frequency. Its symplectic conjugate is then the phase variable $y$ of the polarization state. Both variables characterize a local accessible quantum state. Its *spectral* data including the angular momenta can be recorded by the flat manifolds $\mathcal{O}_\nu$.

In the relativistic hodogram associated to the quantum hologram via the negatively curved eigen time shell attached to the planar coadjoint orbit $\mathcal{O}_\nu$ $(\nu \neq 0)$ of global angular frequency

$$\nu = \frac{2\pi}{T} = \mathrm{Pf}(\lambda_{\mathcal{O}_\nu})\,, \qquad T \neq 0\,,$$

the global radial velocity associated with $\mathcal{O}_\nu$ is defined by

$$v = \tanh \pi\nu = -\mathrm{i}\tan(\mathrm{i}\pi\nu)\,,$$

which is in accordance with the Einstein composition law deduced from the chain rule of cross-ratios in the complex projective plane $\mathbb{CP}^2$. It follows $|v| < 1$, and the Doppler identities

$$\nu = \frac{1}{\pi}\,\mathrm{arctanh}\, v = \frac{1}{2\pi}\log\left(\frac{1+v}{1-v}\right).$$

Then the Laguerre phase formula of the geometry of the complex projective plane $\mathbb{CP}^2$ implies that the hodograph of the Keplerian planetary motion, which forms the orbit inside the planar hodogram, represents a *circle* with radius inversely proportional to the angular momentum. This velocity director circle is actually defined by the central character of $G$ according to the assignment

$$C \ni \begin{pmatrix} 1 & 0 & z \\ 0 & 1 & 0 \\ 0 & 1 & 1 \end{pmatrix} \rightsquigarrow \mathrm{e}^{2\pi \mathrm{i} \nu z}, \qquad \nu = \mathrm{Pf}(\lambda_{\mathcal{O}_\nu}).$$

The synthetic generation of a one-dimensional projective quadric via an orthogonality involution of conjugate lines in the complex projectice metric plane $\mathbb{CP}^2$ [47] establishes that the velocity director circle, together with its orientation, determines uniquely the orbit of the Keplerian planetary motion as well as the *axial* direction of its Laplace or Runge–Lenz vector [61] pointing towards the periastron. Any oriented circle which lies in some plane containing the involution center can occur as a velocity director circle in the planar hodogram. The circles pass through the conjugate cyclic points $\{\bar{\mathrm{i}}, \mathrm{i}\}$ of the complex projective metric plane $\mathbb{CP}^2 \hookrightarrow \mathbb{CP}^3$. Due to the affine classification of the one-dimensional, double point free, central quadrics inside $\mathbb{CP}^2$, the corresponding orbit is associated either with an elliptic, hyperbolic, or parabolic motion according as the involution center lies inside, outside, or exactly on the velocity director circle. Their asymptotes are the tangents through the center at the absolute projective quadric

$$\Phi^\circ_\infty \hookrightarrow \mathbb{CP}^1,$$

and form double lines of the line involution at the center with respect to the one-dimensional projective quadric. They represent the conjugate diameters of the diameter involution which determines the focal points of the one-dimensional central projective quadric in $\mathbb{CP}^2$ by the orthogonality involution of conjugate lines in the complex projective metric plane $\mathbb{CP}^2$. The intersection of the asymptotes is the unique focal point of a circle. It coincides with its center, the center of the diameter involution. Each ellipse which is not a circle, and each hyperbola has four tangents and therefore four focal points. The case of the parabolic motion is distinguished by the fact that the axis of the orthogonality involution, the line at infinity of the complex projective metric plane $\mathbb{CP}^2$ which joins the conjugate cyclic points $\{\bar{\mathrm{i}}, \mathrm{i}\}$, represents a tangential line [47]. In any case, the angle between two radial velocity vectors, as measured around the velocity director circle, is equal to the phase angle between corresponding position vectors.

These important facts on the projective geometry of the Kepler problem have been discovered by Sir William Rowan Hamilton (1805–1865) in 1846 when he studied an alternative for solving dynamical problems [29–31, 44]. They are straightforward within the coadjoint orbit picture of the unitary dual $\hat{G}$ of the Heisenberg nilpotent Lie group $G$ and permit an inclusion of special relativity into geometric quantization.

In polar coordinates of the negatively curved eigen time shell

$$r = \tau \sinh \nu \,, \qquad t = \tau \cosh \nu$$

which is located within the light cone of the Minkowskian spacetime manifold with vertex at the singular plane $\nu = 0$ of "collapsed" singletons, the eigen time parameter $\tau$ satisfies the Minkowskian condition

$$\tau^2 = t^2 - r^2 \,.$$

It is obviously invariant under timelike orthogonality involution with the one-dimensional center $C \hookrightarrow G$ under the logarithmic scale of the real **Heisenberg Lie algebra** $\mathfrak{g}$.

The planar coadjoint orbits $\mathcal{O}_\nu$ belonging to

$$\mathrm{Ad}^*_G(G)\,(\mathbb{R}^\times) \hookrightarrow \mathfrak{g}^\star$$

coincide with the symplectic *leaves* of the Poisson structure of $\mathcal{C}^\infty\,(\mathfrak{g}^\star)$ with Poisson bracket

$$\{f, g\} = c\left(\frac{\partial f}{\partial a}\frac{\partial g}{\partial b} - \frac{\partial f}{\partial b}\frac{\partial g}{\partial a}\right) \,, \qquad a, b, c \in \mathbb{R}$$

for complex-valued functions $f, g \in \mathcal{C}^\infty(\mathfrak{g}^\star)$. The symplectic affine leaves are slicing up the real dual $\mathfrak{g}^\star$ and form the symplectic affine spinorial substrate or synchronized hypostasis of the spatio–temporal *filter bank* implementation of phase *coherent* optics, quantum optics of the matter wavelets of *Bose–Einstein condensates*, astrophysics of *gravitational wavelets* , *quantum information processing*, and phase coherent quantum field theory. As quantum hologram planes, the spectral data slices come in *mirrored* pairs of *absolute* simultaneity

$$(\mathcal{O}_\nu, \mathcal{O}_{-\nu}) \,, \qquad \nu \in \mathbb{R}^\times$$

according to the following non-locality theorem which refers to the concept of complex anti-Hilbert space ( [57]). Each single point in $\mathrm{T}^\star\mathbb{R} \times \{0\}$ forms a *leaf.*

The following result of global Frobenius *reciprocity* type justifies to associate to the planar coadjoint orbits $\mathcal{O}_\nu\,(\nu \neq 0)$, of the unitary dual $\hat{G}$ of the Heisenberg nilpotent Lie group $G$ the compact Kähler manifold $\mathbb{CP}^2$.

**Theorem.** (Antisymmetric Entanglement) *Let $G$ denote a simply connected* nilpotent *Lie group. The following properties of the* ***Schrödinger representation*** $\rho \in \hat{G}$ *and its* ***allied filter bank operators*** *are equivalent:*

i) *The coadjoint orbit $\mathcal{O}_\rho$ forms a symplectic affine* linear *variety of subband coding in the real vector space dual $\mathfrak{g}^\star$;*

ii) *If the one-dimensional identity representation $I$ is* vaguely *contained in the tensor product representation $\rho\hat{\otimes}\sigma$ for $\sigma \in \hat{G}$, then $\sigma = \check{\rho}$ is the contragredient representation of $\rho \in \hat{G}$ acting on an everywhere dense vector subspace of the complex anti-representation Hilbert space of $\rho$.*

The planar coadjoint orbit pairs of absolute simultaneity $(\mathcal{O}_\nu, \mathcal{O}_{-\nu})$ represent the symplectic affine spinorial substrates for the spectral detection of the wavelets of simultaneity [32] at frequencies $\nu \neq 0$. Due to the Laguerre phase formula of the geometry of the complex projective plane $\mathbb{CP}^2$, the synchronization of the planar phase clockwork of the pair of slices $(\mathcal{O}_\nu, \mathcal{O}_{-\nu})$ and their attached eigen time shells by the symmetry of reflection is in accordance with the concept of absolute simultaneity of special relativity theory. The nonlocality can be approved not only by the quantum teleportation phenomenon through EPR information transmission channels but also by quantum optical interference experiments performed with the matter wavelets of Bose–Einstein condensates [6]. In this case, for the spatially coherent wavelets divided by a virtual double slit in a Einstein–Bose bubble of dilute Rb-atomic vapor, the phase in one arm of the interferometer uniquely determines the phase of the other one. The phase coherency of the matter wavelets does not depend upon the distance of the virtual slits of the magnetic trap controlled by radiofrequency waves.

**Corollary.** *The element $\rho \in \hat{G}$ is square integrable modulo its kernel if and only if each element $\sigma \in \hat{G}$ for which $I$ is vaguely contained in $\rho\hat{\otimes}\sigma$ must be equal to $\check{\rho}$.*

The square integrability modulo kernel suggests to emphasize the probabilistic background of the Stone–von Neumann theorem [43], the positive definiteness of the kernel distribution allied to the global Frobenius reciprocity theorem [36, 37, 46], and the Ornstein–Uhlenbeck semigroup of the Bargmann–Fock representation of $G$ [54].

## 4. The Stochastic Realization of the Longitudinal Spectral Flow

The preceding result opens the window to the *stochastic* aspects of the uncertainty principle of quantum information detection, and specifically to the unbiased probability estimate of spatial Lévy stochastic processes [8, 14, 24, 46]. Due to the logarithmic scale of the **real Heisenberg Lie algebra** $\mathfrak{g}$, the principle of maximum Cramér–Rao bound [27] applied to these coherent Markov stochastic processes of *stationary* independent increments along the line bundle of adjoint orbits of $G$ allows to deduce the Schrödinger evolution equation of quantum physics by means of a compromise in the competition between minimizing the Fisher information about the particle's measured position and maximizing its kinetic energy $\mathcal{E} - \Phi$, where $\Phi$ denotes a real-valued, non-temporal,

potential energy function. In the gauge defined by the Bohr–Sommerfeld quantization procedure, the Schrödinger equation [14] provides the probability law of a square integrable wave function $\psi$ such that the probability amplitude

$$p = \sqrt{\psi\bar{\psi}} = |\psi|$$

minimizes the Fisher information [27] of the longitudinal spectral flow

$$\int_{\mathbb{R}} \left( \frac{\mathrm{d}}{\mathrm{d}s} \log p(s) \right)^2 p(s)\, \mathrm{d}s = \int_{\mathbb{R}} \frac{p'(s)^2}{p(s)}\, \mathrm{d}s\,.$$

In the information channel the spectral flow realizes a longitudinal Lévy stochastic process of infinitely divisible *smooth* probability law $p(s)\,\mathrm{d}s$ [50, 28], subject to the mean kinetic energy constraint. Note that the Fisher information reflects the quadratic dilation in the longitudinal direction of $\mathfrak{g}$ and therefore is *different* from the differential entropy. The quantum statistical concept of Cramér–Rao estimator appears to be a more sensitive measure of curve shape and smoothness than the concept of Shannon entropy. Its quantum information theoretical background is able to replace the "incomprehensible" first derivation of the Schrödinger evolution equation discovered by Erwin Schrödinger in 1926, three years after Louis de Broglie modeled a particle as a wavepacket in 1923. The new derivation of the Schrödinger equation is based on the non-trivial *characters*, or non-trivial "singular" unitary linear representations of dimension one of $G$, visualized by the collapsed singletons of the *pointed* singular plane $\nu = 0$ inside the real vector space dual $\mathfrak{g}^\star$ [14].

In classical probability theory, the Lévy–Hinčin formula describes all continuous normalized conditionally positive definite functions on the real line $\mathbb{R}$ [28, 46]. Due to the stochastic definition of $p = |\psi|$, the Lévy–Hinčin spectral trace formula for the characteristic exponent, applied to the *catenation* of the longitudinally *driving* Lévy stochastic process with a Polish space of right continuous paths with left limits, and the *reflected* longitudinal Lévy process, provides a stochastic realization of the sandwich trace configuration of mirrored pairs of planar coadjoint orbits, including the spatio–temporal phase gradient and augmented by an independent pure-jump martingale [53] which represents the channel *noise*. Thus quantum statistics permits to overcome Wolfgang Ernst Pauli's "*difficult* dimensional transition $3 \rightarrow 4$". The random signals associated with the uniquely determined Lévy decomposition [8] into a Brownian motion with drift, a compound Poisson stochastic process, and a martingale, which is created by the standard *cascade* of slices, undergo a *matched* filtering process. At optical frequencies, the coherent wavelets associated to the compound Poisson stochastic process are generated by the field of a *laser* above threshold. In

this stochastic framework of geometric quantization, Niels Bohr's complimentary principle of quantum physics adopts a simple geometric meaning within $\mathfrak{g}^\star$, and the Schrödinger equation exhibits to be complimentary to the Lorentz invariant Klein–Gordon equation (Section 12 infra).

In the context of phase coherent quantum field theory, two remarks are in order:

1. A consequence of the stochastic modality that is of methodological as well as historical importance is the fact that the Keplerian laws of planetary motion can be deduced independently of Newton's gravitational law. This consistency was well known to the philosopher Georg Wilhelm Friedrich Hegel (1770–1831), but most of the post-Newtonian physicists and philosophers like Karl Raimund Popper have not been aware of this astrophysical insight [48]. Indeed, central projective homogenization of the Lévy intensity measure provides the Third Keplerian Law. This result provides a new probabilistic perspective "more geometrico" of the gravitational law.
2. The trace of the longitudinal evolution operator associated to the Schrödinger equation leads to the Landsberg–Schaar identity for quadratic Gaussian sums

$$\frac{1}{\sqrt{p}} \sum_{0\leq n\leq p-1} e^{2\pi \mathrm{i}\frac{n^2 q}{p}} = \frac{1}{\sqrt{2q}}\, \mathrm{e}^{\frac{\pi \mathrm{i}}{4}} \sum_{0\leq n\leq 2q-1} \mathrm{e}^{-\pi \mathrm{i}\frac{n^2 p}{2q}}\,, \qquad p>0,\, q>0$$

valid for *positive* integers $p$ and $q$ [7, 15]. In number theory, this identity which includes the Maslov index plays a central role underpinning key results relating to the quadratic reciprocity law in terms of Legendre symbols

$$\left(\frac{p}{q}\right)\left(\frac{q}{p}\right) = (-1)^{\frac{p-1}{2}\,\frac{q-1}{2}}$$

for *odd* integers $p$ and $q$, and characters. An alternative way of establishing the Landsberg–Schaar identity depends upon path integration of the longitudinally driving Lévy stochastic process and the reflected longitudinal Lévy process [16]. Shor's algorithm for quantum computation actually suggests a close interrelation between number theory and quantum information.

## 5. The Hopf and the Contragredient Hopf Fiber Bundle

The stereographic projection

$$\bar{\gamma}\colon \mathbb{S}^2\backslash\{\text{north pole}\} \longrightarrow \mathcal{O}_1$$

known already to Ptolemy as a conformal mapping endowes the complex projective line $\mathbb{S}^2 = \mathbb{CP}^1 \hookrightarrow \mathbb{CP}^2$ with the curvature form of the linear connection

$P$ of the $\mathbb{S}^1$ principal fiber bundle

$$\pi\colon \mathbb{S}^3 = \{(w_1, w_2) \in \mathbb{C}^2;\ |w_1|^2 + |w_2|^2 = 1\} \longrightarrow \mathbb{S}^2 = \mathbb{CP}^1$$

with $\mathbb{S}^1$ action

$$(w_1, w_2)\,.z = (w_1.z, w_2.z)\,.$$

Then the exterior differential 1-form $P$ on $\mathbb{S}^3$ with values in the Lie algebra $\mathrm{T}_1\mathbb{S}^1 = \mathrm{i}\mathbb{R}$ of the one-dimensional torus group $\mathbb{T} = \mathbb{R}/\mathbb{Z}$ takes the form

$$P = \frac{1}{2}\left(\bar{w}_1\,\mathrm{d}w_1 - w_1\,\mathrm{d}\bar{w}_1 + \bar{w}_2\,\mathrm{d}w_2 - w_2\,\mathrm{d}\bar{w}_2\right)$$

and $\Omega = \mathrm{d}P$ is the closed exterior differential (1,1)-form

$$\Omega = -\left(\mathrm{d}w_1 \wedge \mathrm{d}\bar{w}_1 + \mathrm{d}w_2 \wedge \mathrm{d}\bar{w}_2\right)$$

on $\mathbb{S}^3$ with values in $\mathrm{T}_1\mathbb{S}^1 = i\mathbb{R}$. Let $\bar{\Omega}$ denote the exterior differential (1,1)-form on $\mathbb{S}^2 = \mathbb{CP}^1$ so that $\Omega = \pi^\star\bar{\Omega}$. Let $\bar{\bar{\Omega}}$ denote an exterior differential (1,1)-form on $\mathbb{C}$ so that

$$\bar{\gamma}^\star\bar{\bar{\Omega}} = \bar{\Omega}$$

holds. Then the mapping

$$\bar{\gamma} \circ \pi\colon \mathbb{S}^3 - \{(w_1, w_2);\ w_2 \neq 0\} \longrightarrow \mathbb{C}$$

takes the explicit form of a homogeneous coordinatization

$$\bar{\gamma} \circ \pi(w_1, w_2) = \frac{w_1}{w_2}\,,$$

and therefore projects every circle on the unit sphere $\mathbb{S}^3 \hookrightarrow \mathbb{C}^2$ onto a circle or line in the complex plane $\mathbb{C}$. It follows that $\mathbb{S}^3$ forms a circle bundle over $\mathbb{CP}^1$, and that $\bar{\bar{\Omega}}$ is given by

$$\bar{\bar{\Omega}} = -\frac{\mathrm{d}w \wedge \mathrm{d}\bar{w}}{\left(1 + |w|^2\right)^2}\,.$$

Moreover, it follows from the surface integral

$$\frac{1}{2\pi\mathrm{i}} \int\limits_{\mathbb{S}^2} \bar{\Omega} = 1$$

that the Chern class of the Hopf bundle takes the form

$$c_1\,(\text{Hopf bundle}) = -1\,.$$

By choosing a copy of $\mathbb{C}$ inside the skew-field $\mathbb{H}$ of Hamiltonian quaternions, the one-dimensional torus group $\mathbb{T} = \mathbb{S}^1$ can be identified with a subgroup of $\mathbb{S}^3$. The fibers of the Hopf bundle

$$\begin{array}{ccc} \mathbb{S}^1 & \longrightarrow & \mathbb{S}^3 \\ & & \downarrow \\ & & \mathbb{S}^2 \end{array}$$

correspond to the places where the ratio $w_1/w_2$ is constant. The fibers over the north and south poles are the longitudinal axis and the central circle. All but two of the fibers of the Hopf bundle are located on the foliating tori lying over the lines of latitude on the unit sphere $\mathbb{S}^2 \hookrightarrow \mathbb{R}^3$ [10] as Villarceau circles. On each torus the fibers run around once in each direction of the Villarceau circles. The base manifold $\mathbb{S}^2$ may be regarded as the space of fibers in the sense that the projection $\pi$ establishes a bijection between the set of fibers and the base. Moreover, the topology on the base manifold indicates the mutual disposition of the fibers in the sense that two fibers are near each other when the corresponding base points are near each other. The space of fibers is made up of two two-dimensional compact discs glued together by a diffeomorphism of their boundaries, which is just the unit sphere $\mathbb{S}^2 \hookrightarrow \mathbb{R}^3$. Therefore the group of Lorentz transformations as a group of rotational collineations of $\mathbb{CP}^2$ respects the Hopf fibration as well as the Bohr–Sommerfeld quantization procedure. In terms of Johannes Kepler, "Geometria est archetypus of pulchritudinis mundi". In a similar vein, the $\mathbb{S}^1$ action $\mathbb{S}^3 \times \mathbb{S}^1 \longrightarrow \mathbb{S}^3$ defined by the assignment

$$(w_1, w_2).z^{-1} = (w_1.z^{-1}, w_2.z^{-1})$$

and the contragredient stereographic projection

$$\underline{\gamma}\colon \mathbb{S}^2 \backslash \{\text{south pole}\} \longrightarrow \mathcal{O}_{-1}$$

as a conformal mapping combine so that the transformation

$$\underline{\gamma} \circ \pi\colon \mathbb{S}^3 - \{(w_1, w_2);\, w_1 \neq 0\} \longrightarrow \mathbb{C}$$

arises. The coordinate chart compatibility

$$\underline{\gamma} \circ \pi(w_1, w_2) = \frac{w_2}{w_1} = \left(\frac{w_1}{w_2}\right)^{-1} = (\bar{\gamma} \circ \pi(w_1, w_2))^{-1}$$

provides the contragredient Hopf bundle of principal linear connection

$$-P\colon \mathrm{T}\mathbb{S}^3 \longrightarrow \mathrm{i}\mathbb{R}\,.$$

It follows

$$\underline{\Omega} = -\,\mathrm{d}P = -\Omega = \mathrm{d}w_1 \wedge \mathrm{d}\bar{w}_1 + \mathrm{d}w_2 \wedge \mathrm{d}\bar{w}_2\,,$$

so that

$$\underline{\bar{\Omega}} = -\bar{\Omega} = \frac{\mathrm{d}w \wedge \mathrm{d}\bar{w}}{(1 + |w|^2)^2}\,,$$

via the surface integral

$$\frac{1}{2\pi \mathrm{i}} \int\limits_{\mathbb{S}^2} \underline{\bar{\Omega}} = -1 \,,$$

yields the Chern class

$$c_1(\text{contragredient Hopf bundle}) = +1 \,.$$

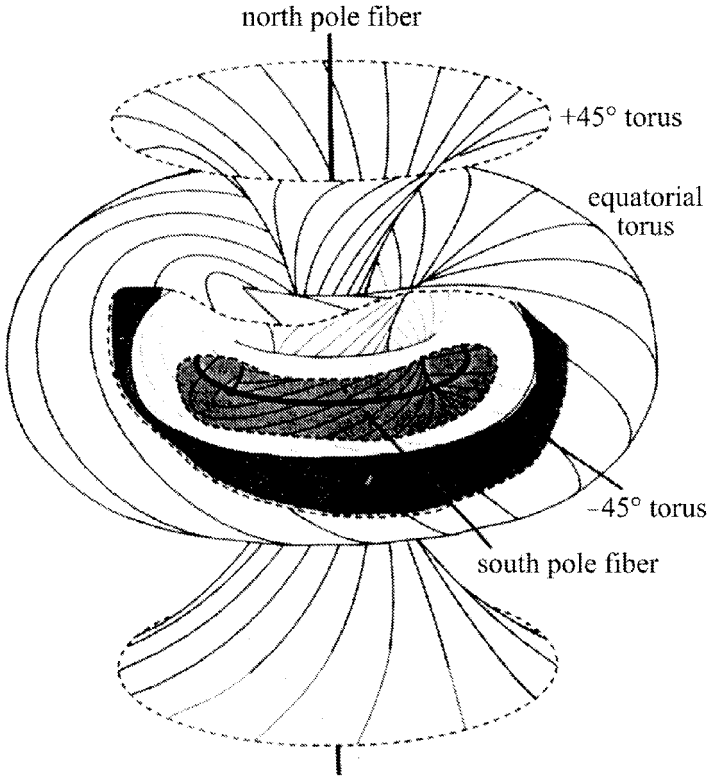


**Figure 3.** A cutaway perspective view of the Hopf fibration on $\mathbb{S}^3 \hookrightarrow \mathbb{R}^4$
The fibers on the three compact tori which consist of Villarceau circles lying over the equator, and the $\mp 45$ degree parallels of the unit sphere $\mathbb{S}^2 \hookrightarrow \mathbb{R}^3$ are visible. The fibers over the north and south poles, the longitudinal axis and the central circle, are also shown. The space of fibers is made up of two two-dimensional discs glued together by a diffeomorphism of their boundaries, which is just the sphere $\mathbb{S}^2$. Therefore the group of Lorentz transformations as a group of rotational collineations of $\mathbb{CP}^2$ respects the Hopf fibration as well as the Bohr–Sommerfeld quantization procedure. Remarkably, the Hopf fibration corresponds to Kant's absolute epistemologic metaphor of knowledge and visualizes Pauli's "difficult dimensional transition $3 \rightarrow 4$". It leads to the "representatio" of the phenomena in the sense of Kant's epistemologic philosophy of the phenomenon of time, and to the epistemologic metaphor of the "globus intellectualis" introduced into philosophy by Francis Bacon. In terms of Kepler, "Geometria est archetypus pulchritudinis mundi".

On the foliating tori lying over the lines of latitude on the unit sphere $\mathbb{S}^2 \hookrightarrow \mathbb{R}^3$, the fibers run around in the opposite direction than the Villarceau circles of the Hopf bundle. Note that the Hopf fibration forms a visualization of Pauli's "difficult dimensional transition $3 \rightarrow 4$". In special relativity, the dimensional transition $3 \rightarrow 4$ is projectively performed by considering the Lorentz transformations as a group of rotational collineations of the complex projective plane $\mathbb{CP}^2$.

The Chern class involution of the non-isomorphic Hopf fibrations of $\mathbb{S}^3 \hookrightarrow \mathbb{C}^2$ over the complex projective line $\mathbb{CP}^1 = \mathbb{S}^2$ with fiber type $\mathbb{S}^1 \hookrightarrow \mathbb{C}$ is induced by the winding numbers $\{-1, +1\}$ of the respective Villarceau circles. It reflects the basic antisymmetry of the compact Kähler manifold $\mathbb{CP}^2$, implemented by the antisymmetric entanglement theorem as well as the concept of absolute simultaneity of special relativity. It forms the basis of the spin echo technique of MR spectroscopy and the clinical MRI modality because it permits to overcome the decoherence tendency of "hot" organisms.

Ironically enough, the basic antisymmetry of the complex projective plane $\mathbb{CP}^2$ provides also the quantum mechanically derivation of the Einstein equivalence [58]

$$\mathcal{E} = mc^2\,, \qquad m = \frac{m_0}{\sqrt{1 - \frac{v^2}{c^2}}}\,, \qquad |v| < c$$

of radiation energy

$$\mathcal{E} = h\nu\,,$$

and associated mass

$$m = \frac{h\nu}{c^2}\,.$$

Of course, $h = 2\pi\hbar$ denotes Planck's universal constant. The proof depends on the timelike orthogonality involution of the Lorentz transformations and is based on the Third Keplerian Law of planetary motion to introduce the concept of mass $m$ via an appropriate gauge [11]. At rest, in a spacetime splitting so that $v = 0$, the energy is $\mathcal{E} = m_0 c^2$.

A familiar but *incorrect* version of the Third Keplerian Law of planetary motion asserts that the period is proportional to the $\frac{3}{2}$ power of the mean distance from the origin. It is noteworthy that the period of such a periodic orbit depends only on the energy $\mathcal{E}$. Therefore the Third Keplerian Law can be derived "more geometrico" also from the Lévy intensity measure.

The spectral detection by laser interferometry of the emitted gravitational wavelets needs to optically measure relative changes of length at the order

of $10^{-21}$. This distance corresponds to the diameter of a hydrogen atom relative to the distance between Earth and Sun. The photon recycling technique uses the beam splitter and mirrors of a Michelson interferometer as test masses for the gravitons of spin 2. The Chern class involution provides an *enhanced* signal amplitude within the laser interferometer. As in the photon entanglement experiments, the directions of polarization with the conjugate *isotropic* lines as a reference frame are determined by the Laguerre phase formula of the geometry of the complex projective plane $\mathbb{CP}^2$. Due to its interpretation in terms of the radial *relativistic* Doppler filter bank effect of multirate signal analysis or subband coding, the preceding reasoning demonstrates that the Laguerre phase formula is at the *interface* of quantum physics and the special theory of relativity. In particular, Planck's hypothesis concerning the existence of the universal constant $h$ is a direct *consequence* of the Third Keplerian Law of planetary motion. It confirms that this interface is a fascinating topic of projective metric geometry and mathematical physics with highly interesting relations to Kant's epistemology, and the epistemologic metaphor of the "globus intellectualis" introduced into philosophy by Francis Bacon. In geophilosophy, the earth is not one element among others but rather brings together all the elements within a single embrace while using one or another of them to deterritorialize territory. Movements of deterritorialization are inseparable from territories that open themselves, and the process of reterritorialization is inseparable from the earth which restores territories. Territory and earth are two components with two zones of indescernibility: Deterritorialization from territory to the earth, and reterritorialization from earth to territory.

Lightlike straight lines represent information transmission channels. They provide the Lorentz transformations as a Lie group of rotational collineations the actions of which on the conformally invariant two-dimensional sphere $\sqrt{2\pi|\nu|}\,.\,\mathbb{S}^2$ are based on the Fitzgerald–Lorentz contraction. The relativistic hodographs represent the traces of the rotational collineations of $\mathbb{CP}^2$.

A direct consequence of these relativistic reasonings is the gravitational *red* shift. The laboratory experiment by R. V. Pound and G. A. Rebka Jr (1960) as well as the maser experiment performed in a rocket by R. F. C. Vessot (1979) are in good agreement with the theoretically derived results.

## 6. The Metaplectic Representation

The two-fold covering group $Mp(2,\mathbb{R})$ of the real symplectic or special real linear group $Sp(2,\mathbb{R}) = SL(2,\mathbb{R})$ exists because the fundamental group of $SL(2,\mathbb{R})$ is the cyclic group $\mathbb{Z}$. It contains the central subgroup $\mathbb{Z}_2$ isomorphic

to the cyclic group $\mathbb{Z}/2\mathbb{Z}$ of order 2 such that

$$Mp(2,\mathbb{R})/\mathbb{Z}_2 = Sp(2,\mathbb{R})$$

and $Mp(2,\mathbb{R})$ is a non-trivial extension of $Sp(2,\mathbb{R})$ by $\mathbb{Z}_2$ in the sense that it is *not* the direct product $Sp(2,\mathbb{R}) \times \mathbb{Z}_2$. One may regard the standard representation $\rho$ of $G$ as a representation of the semidirect product of $Mp(2,\mathbb{R})$ and $G$.

The metaplectic representation $\omega$ of the metaplectic group

$$\begin{array}{ccc} \mathbb{Z}_2 & \longrightarrow & Mp(2,\mathbb{R}) \\ & & \downarrow \\ & & Sp(2,\mathbb{R}) \end{array}$$

acts on the standard complex Hilbert space $L^2(\mathbb{R})$ as an irreducible unitary linear representation. Its normalization action is defined via the covariance identity

$$\omega\left(\tilde{\alpha}\right)\rho(g)\omega\left(\tilde{\alpha}\right)^{-1} = \rho\left(\alpha(g)\right)$$

for all elements $g \in G$ where the basepoint projection $\tilde{\alpha} \rightsquigarrow \alpha$ maps the metaplectic group $Mp(2,\mathbb{R})$ onto the base manifold $Sp(2,\mathbb{R}) = SL(2,\mathbb{R})$. The point to note is that it is this mapping which indicates in the quantum teleportation problem that antisymmetrically polarization-entangled photon pairs can reproduce quantum information transmitted *instantaneously* to a remote location via EPR information transmission channels because $\omega\left(\tilde{\alpha}\right)$ where $\alpha$ are phases in the subgroup $SO(2,\mathbb{R})$ of the group of automorphisms $SL(2,\mathbb{R})$ of $G$ allows to perform instantaneously changes of the polarization state by antisymmetric continuous phase shifts in the relativistic trajectories of a photon pair interferometer which preserves the moments. The fact that

$$\begin{array}{ccc} \mathbb{Z}/2\mathbb{Z} & \longrightarrow & Mp(2,\mathbb{R}) \\ & & \downarrow \\ & & SL(2,\mathbb{R}) \end{array}$$

forms a two-fold covering group of the real symplectic group $Sp(2,\mathbb{R}) = SL(2,\mathbb{R})$ implies via the Maslov index [58] a violation of Bell's inequality for certain states of polarization.

Antisymmetrically polarization-entangled photon pairs cannot perfectly clone the information which has been transmitted [9] so that there is an aspect of *undecidability* in the transmission of quantum information to remote locations via EPR information transmission channels. Due to the non-cloning theorem, quantum physics is *not* in conflict with relativity theory, even for tachyons.

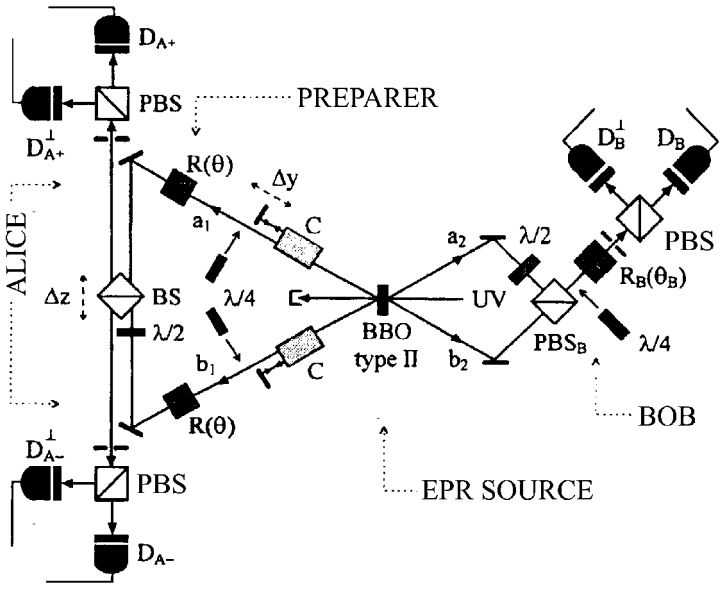


**Figure 4.** Visualization of the global Frobenius reciprocity
Quantum teleportation in a photon pair interferometer which preserves the moments. The EPR source spatially separates the quantum teleportation system into two remote subsystems. The photon trajectories of the left hand subsystem represent the preparing procedure of the spectral object. It allows to perform phase shifts by the action of the metaplectic representation $\omega$. The left hand side subsystem forms the cohomological aspect of the chirality experiment. Calcite crystals (C) are acting as double refracting polarizers which separate horizontally and vertically polarized photons. The photon trajectories on the right hand side represent the sandwich trace configuration of mirrored pairs of planar coadjoint orbits $(\mathcal{O}_\nu, \mathcal{O}_{-\nu})$ which permit to acquire the phase shifts. The right hand side subsystem forms the cohomotopic aspect of the experiment. Both sides are non-locally coupled by the antisymmetric entanglement process of photonics (BS = beam splitter, D = detector).

In the quantum teleportation experiment, a transmitter, traditionally called Alice, is given a quantum state unknown to her. She also has one photon of a photon pair prepared in an EPR state by path entanglement. She performs a Bell measurement on the combined system consisting of the unknown state and her EPR photon, and then transmits the result of the measurement via a classical information channel to the receiver Bob, who has the second of the EPR photon pair. Depending on the result of the measurement, Bob performs one of the four possible unitary linear transformations on his photon and it will now be in the unknown state. If the preparer does not inform Alice about what quantum state he has prepared then there is no way she can find out what the quantum state actually is.

## 7. Microwave Holography: Synthetic Aperture Radar Imaging

The synthetic aperture principle based on a small antenna simulating a larger one, can be regarded as a subcase of the broader range Doppler principle which is one of the basic pillars of microwave radar technology and relativistic radial measurements of the pulsar clockwork. The function of the antenna is to coherently detect the signal impinging on each element and to superimpose these signals by respecting their phases. For microwave SAR, the echo received at a particular aperture location results from energy transmitted from that known location in the aperture, that is, more information is received by the SAR hardware than for a real aperture radar (RAR) system [63]. It has been observed by Carl Wiley of the Goodyear Corporation in 1951 that the resolution for a microwave SAR is finer than the resolution for a RAR of equal aperture. His design is today referred to as squint mode SAR [20].

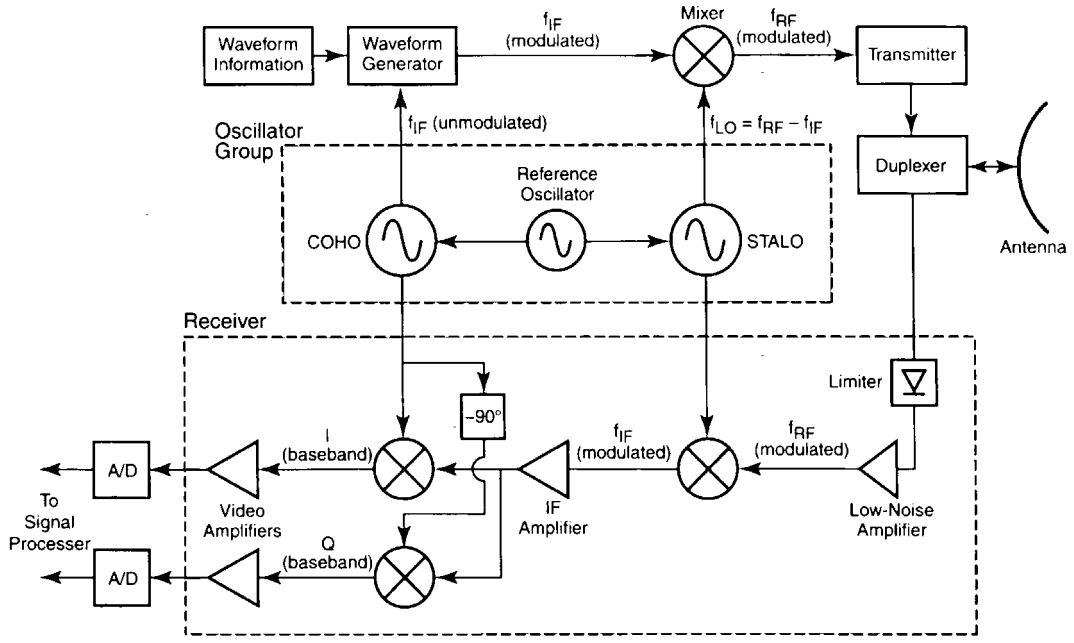


**Figure 5.** Simplified block diagram of a coherent radar system
The oscillator group provides coherent signals via mixers which are indicated by the symbol $\otimes$. In the receiver, the phase delay of $-90$ degrees implements the symplectic structure of the coadjoint orbit of holographic imagery $f_{IF}$ = intermediate frequency, $f_{RF}$ = radio frequency, COHO = coherent oscillator, LO = local oscillator, STALO = stable local oscillator). The two output channels of the receiver feed A/D converters.

The most famous *microwave* holograms were formed without the process being thought of as a holographic method. Regarding the microwave SAR imaging process in combination with optical processing as microwave holography turns

out to be immensely useful [38, 40]. If the record is treated as a photonic hologram [39], and illuminated with a beam of phase coherent radiation, the customary true and conjugate image fields obtain. Each field is an optical reconstruction, miniaturized by the scaling procedure, of the original radar field sensed by the radar receiver. Each image point is an optical image of an original object point which had been microwave radar illuminated, and having resolution corresponding to the full aperture generated by the scanning antenna. Thus the holographic procedure of remote sensing reconstructs in accordance with the *synthetic* aperture, *not* the actual one.

**Figure 6.** High resolution microwave radar image of the Baltimore–Washington International (BWI) Airport obtained with a microwave SAR modality designed for an unmanned aerial vehicle. The holographic signal processing makes the resolution independent of the sensor's altitude

The physical insight into microwave SAR imaging provided by the holographic viewpoint has led to ideas that otherwise would perhaps never been conceived. The tilted plane optical processor is one such example [38, 40]. In contemporary microwave SAR imaging, the data processing is *digitally* performed [18, 20]. Nevertheless the Heisenberg Lie group approach is still appropriate because its *trace formulae* [34] provide the interpretation of the cross-correlations as the

coefficient functions of the representation class $\rho \in \hat{G}$ modulo $C$. Another consequence is the fact that the generation of chirp signals by the metaplectic representation $\omega$ of the metaplectic group $Mp(2,\mathbb{R})$, and the mixer devices play a dominant role in SAR hardware. It is common for a coherent radar to employ a *quadrature* mixer in which the intermediate frequency signal from the coherent oscillator is mixed with the intermediate frequency signal from the coherent oscillator shifted in *phase* by 90 degrees. Then the output is mixed with the analog signal at baseband. The next mixer combines the output with the stable local oscillator, the STALO in the radar jargon, to produce a low power version of the transmitted signal at the carrier frequency. The outputs of the baseband mixer are routed through video amplifiers and then sampled via A/D converters. The resulting digital signals, often called the video phase history, are used for subsequent signal processing.

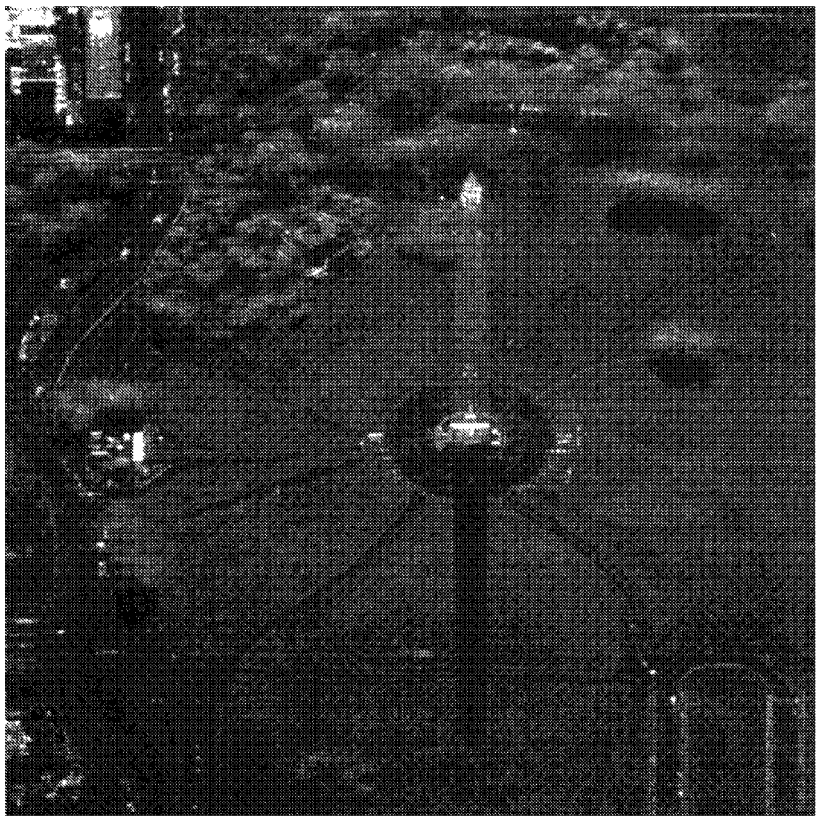

**Figure 7.** Microwave SAR imaging of the Washington Monument
It is a remarkable fact that the resolution is independent of the sensor's altitude. Therefore the figure does not look entirely like an optical image, nor should it. The radar shadow cast by the SAR itself is the most striking feature of the high resolution airborne microwave radar image.

## 8. Clinical Magnetic Resonance Tomography

It should be observed that the diagnostic part of medicine has gone through a revolution in the last few decades, primarily due to the improvements in computer technology. The computationally supported diagnostic facilities have culminated in the clinical modality of MRI. Few techniques involving sophisticated instrumentation have made so rapid an impact on medical diagnosis as has clinical MRI. Emerged as the most powerful diagnostic imaging technique in clinical practice, the MRI modality has rapidly replaced very invasive and less diagnostic methods such as pneumoencephalography, meyelography, and nuclear medicine brain scans. MRI is the premier clinical method for the diagnosis of disease in the central nervous system, because of its speed, noninvasiveness, and capability to create tomograms with exquisite contrast. Presently clinical MRI scanners are ubiquitous and able to cover the full range of all organs of the human body [23, 51, 59].

Although there are very few disorders for which the contributions of the MRI modality may not be important, its most valuable contribution lies in the field of neuroscience. Since early clinical applications of MRI, there has been a growing awareness of its *unique* role in the field of neurotology, in particular, and other fields related to laryngology, and head and neck surgery. MRI has shown its value in supplementing or at times replacing computed tomography (CT) in studying many otological problems. It has become an invaluable tool in studying neurotological disorders. MRI is the study of choice for evaluation of the membranous labyrinth, neurovascular structures of the internal auditory canal, posterior fossa, and central neurotological and vestibular disorders. Early experience with MR angiography quickly proved that it was superior to CT for assessing blood vessels. The capability for studying blood flow with MRI has led to the development of newer techniques such as flow compensation, radio frequency presaturation, three-dimensional MR angiography, sequential slice two-dimensional MR angiography, a combination of three-dimensional MR angiography and double-dose gadolinium enhanced MRI, and innovative techniques such as time resolved contrast enhanced MR angiography which markedly enhanced the field of MR angiography. MR angiography not only permits study of the vascular anatomy, but also shows vessel patency and direction of flow and quantifies flow velocities and volume. New developments to improve the precision for diagnosing pathological changes are ongoing. Neurofunctional MRI and MR spectroscopy are being used in many clinical centers for functional and in vivo analysis of chemical characteristics of disease states [58, 12].

In correspondence to the zero-dimensional absolute projective quadric $\Phi^{\circ}_{\infty} \hookrightarrow$

$\mathbb{CP}^1$ which consists of the conjugate cyclic points

$$\Phi_\infty^\circ = \{\bar{\mathrm{i}}, \mathrm{i}\}$$

joined by the line at infinity of the complex projective plane $\mathbb{CP}^2$ and common, as a phase reference, to all circles of the symplectic affine plane $\mathbb{R} \oplus \mathbb{R}$ as well as to the relativistic hodogram, the traceless matrices

$$J^{-1} = \begin{pmatrix} 0 & 1 \\ -1 & 0 \end{pmatrix}$$

and

$$J = \begin{pmatrix} 0 & -1 \\ 1 & 0 \end{pmatrix}$$

introduce the Fourier transformer $\mathcal{F}_\mathbb{R}$ *and* the Fourier cotransformer $\bar{\mathcal{F}}_\mathbb{R}$, respectively. These transformers are acting on the complex Schwartz space $\mathcal{S}(\mathbb{R}) \hookrightarrow L^2(\mathbb{R})$ on the real line $\mathbb{R}$. They are associated to the metaplectic representation $\omega$ of the metaplectic group $Mp(2, \mathbb{R})$ via the normalization relations

$$\omega(J^{-1}) = \mathcal{F}_\mathbb{R}\,, \qquad \omega(J) = \bar{\mathcal{F}}_\mathbb{R}\,.$$

Thus the natural symplectic structure of the planar coadjoint orbits $\mathcal{O}_\nu$ $(\nu \neq 0)$ and its orthogonality involution of conjugate lines in the complex projective metric plane $\mathbb{CP}^2$ gives not only rise to the real focal points of the elliptic, hyperbolic and parabolic motions and the axial direction of the Runge–Lenz vector associated to the dynamical system, but also to the Fourier transformer and co-transformer which correspond to the non-real foci of the elliptic and hyperbolic orbits in the Keplerian conchoid construction of the First Law of planetary motion [56, 60].

The intertwiners exhibit $x$ as a phase variable and $y$ as a spatial frequency variable [54]. The symplectic Fourier transformer

$$\mathcal{F}_{\mathbb{R} \oplus \mathbb{R}} = \mathcal{F}_\mathbb{R} \wedge \bar{\mathcal{F}}_\mathbb{R}$$

is of order 2 instead of order 4 because only two lightlike isotropic tangents drawn from the conjugate cyclic points $\Phi_\infty^\circ = \{\bar{\mathrm{i}}, \mathrm{i}\}$ to the one-dimensional absolute central projective quadric of special relativity

$$\Phi_\infty \hookrightarrow \mathbb{CP}^2$$

are activated. Besides the orthogonality involution of the rotational collineations of the complex projective plane $\mathbb{CP}^2$ which induce the group of Lorentz transformations via the Fitzgerald–Lorentz contraction, it provides the filter bank implementation for the generation of the final image of observation [25].

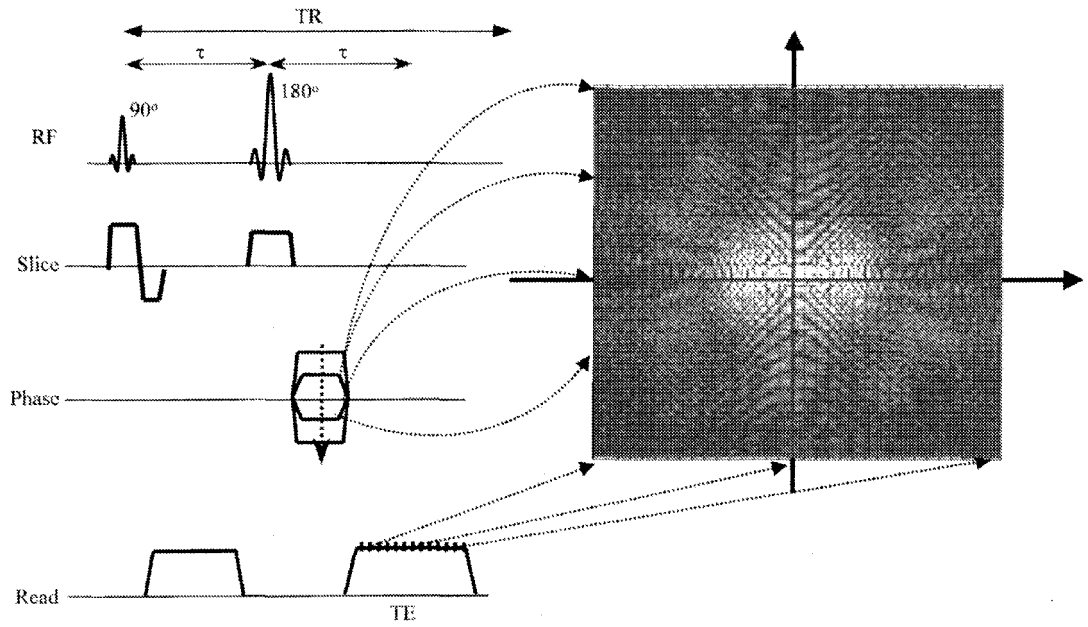


**Figure 8.** The spatio–temporal phase encoding gradient controls which row of the quantum hologram is collected, whereas the sampling of the induced voltage determines which data of each row is collected. The figure displays the spatio–temporal phase encoding gradient that controls the row, the data sampling during the spatio-temporal frequency encoding procedure that determines the position along the row, and the appearance of the MRI raw database forming the quantum hologram before its symplectic Fourier transform reconstruction. It is the phenomenon of the invisible time axis which solves the non-local binding problem of MRI by synchronization.

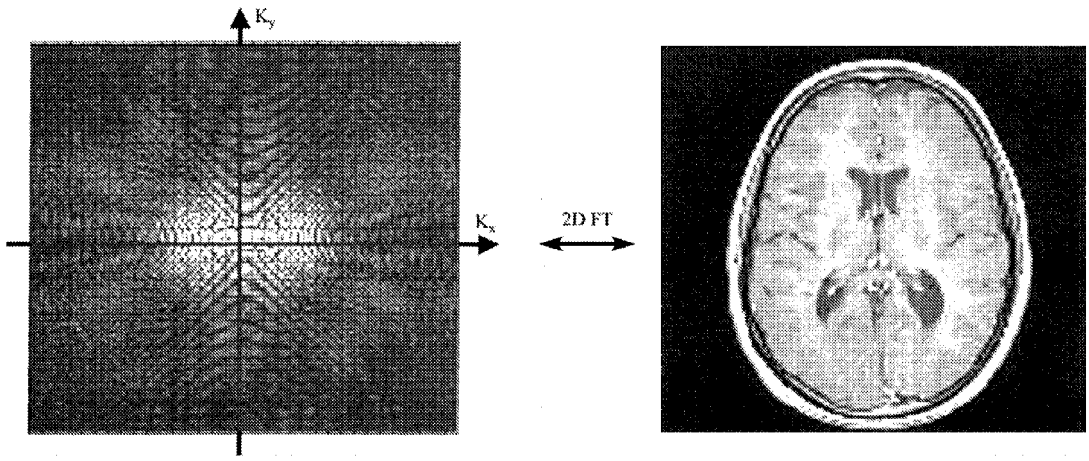


**Figure 9.** A full sampling of the quantum hologram allows a symplectic Fourier transform reconstruction: The application of the symplectic Fourier transformer $\mathcal{F}_{\mathbb{R}\oplus\mathbb{R}}$ generates the final image. It is the phenomenon of time which solves the non-local binding problem of MRI by synchronization. In the hardware of clinical MRI scanners, the fast symplectic Fourier transformer is implemented by a special-purpose processor.

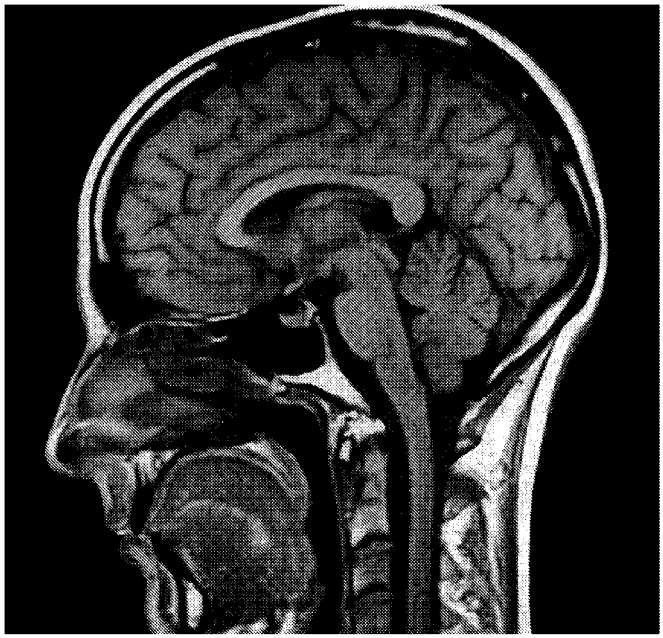

**Figure 10.** High resolution clinical magnetic resonance tomography
Sagittal cross-section of the neurocranium along the falx cerebri within the longitudinal interhemispheric fissure demonstrating midline sagittal neuroanatomy of the outwardly rounded gyri and inwardly invaginating fissures and sulci of the human brain. The various portions of the corpus callosum shown include the rostrum, genu, body and splenium, pineal gland, quadrigeminal plate, infundibulum, third and fourth ventricle, pituitary gland, cerebellar vermis, pons, aqueduct of Sylvius prepontine space, and craniocervical junction. High resolution MRI scans approximate the same level of detail as cut specimens to depict neuroanatomy even in the deepest recesses of the brain.

An alternative encoding method to the symplectic Fourier transform MRI is wavelet encoding. Wavelet encoding approaches the resolution limit defined by the Fourier encoding procedure [45].

Finally, it should be emphasized that the idea of creating time by imaging is already in Kant's "repraesentatio" of the phenomena. Actually, some of his ideas on physical time as explained in *"De mundi sensibilis atque intelligibilis forma et principiis"* can be traced back to Leibniz, and even Platon's philosophy of the phenomenon of time. It is the phenomenon of time which solves the non-local *binding* problem of imaging by synchronization.

## 9. The DNA Double Helix Configuration

Virtually all explicitly known solutions of Einstein's field equations for physically plausible matter fields admit a high degree of dynamical symmetry. This holds for the Schwarzschild, Kruskal, and Kerr solutions [33, 17]. Spherically symmetric spacetime manifolds provide excellent descriptions of non-rotating,

isolated stars and therefore are of astrophysical interest. If the star rotates, the rotation axis breaks the dynamical symmetry.

The spectral detection of gravitational wavelets suggests to apply the geometry of the Heisenberg group $G$ to cosmology [26]. From geometric control theory it is known that the Lie group $G$ under its natural spatial metric serves as a paradigm for a Carnot–Carathéodory manifold exhibiting the role of non-holonomy. Its geodesic flow is defined by the Heisenberg helices [58]

$$\begin{pmatrix} 1 & \frac{-x(1-\cos 2\pi\nu t)-y\sin 2\pi\nu t}{2\pi\nu} & \frac{(x^2+y^2)(2\pi\nu t-\sin 2\pi\nu t)}{2(2\pi\nu)^2} \\ 0 & 1 & \frac{x\sin 2\pi\nu t-y(1-\cos 2\pi\nu t)}{2\pi\nu} \\ 0 & 0 & 1 \end{pmatrix}, \qquad t\in\mathbb{R}\,.$$

The Heisenberg helices are, considered as geodesics of the sub-Riemannian geometry of $G$ starting at the origin, the solutions of the associated Hamiltonian equations [58, 57]. In molecular genetic information processing, their reflection corresponds to the concept of antiparallel stereochemical base complementarity in the (A • T; G • C) alphabet of nucleotide sequences, discovered by Erwin Chargaff in 1950 on the basis of Friedrich Miescher's nucleic acid paradigm. The double helix model of the molecular structure of DNA discovered by Francis H. Crick and James D. Watson (Nobel prize 1962) finally emerges from the basic principle of antisymmetry of the Heisenberg helix which has its longitudinal counterpart in the Plancherel measure on the timelike center $C \hookrightarrow G$, and its transversal counterpart in the Kähler metric of the complex projective hyperplane $\mathbb{CP}^2 \hookrightarrow \mathbb{CP}^3$. Due to the antiparallel orientation of the *base-pairing*, the holographic transform of the nucleic acid information carriers provides the perfect *semi-conservative* replication process of molecular genetics.

Recently the energy stereochemically stored in the double DNA helix allowed to genetically construct mechanical machines at the nano scale such as a pair of DNA tweezers. The length of the complementary base-pairs of the double helices is less than 7 nm.

## 10. The Kruskal Diagram of Cosmology

The unit sphere is the image of a geodesically *incomplete* Lorentz invariant circular cylinder of radius $r = \sqrt{x^2+y^2}$ under its combined stationary and axial symmetry actions. The minimizing geodesics supported by the circular energy cylinder derive from the classical isoperimetric problem of the Euclidean plane $\mathbb{R}^2$. The pullback of the Einstein cylinder world lines or photon trajectories of relativity theory to the spheres in spacetime define the Kruskal coordinatized two-fold covered Minkowskian spacetime manifold of Clifford

algebra $\mathcal{C}\ell(3,1,\mathbb{R})$ in which radial light rays everywhere have the slope $\pm 1$. Because the one-dimensional absolute central projective quadric $\Phi_\infty \hookrightarrow \mathbb{CP}^2$ is common to all Euclidean spheres of $\mathbb{R}^3$, an application of the canonical Kustaanheimo–Stiefel transformation of spinorial celestial mechanics [61, 62], combined with the correct gravitational potential in the exterior region, directly yields the spherical symmetric two-fold covering of the Schwarzschild manifold. Notice also that the geometry of the Kustaanheimo–Stiefel transformation implements the axial direction of the Runge–Lenz vector.

The canonical Kustaanheimo–Stiefel transformation exhibits to form an orbit under the natural conjugation action of the skew-field $\mathbb{H}$ on $\Phi_\infty^\circ \hookrightarrow \Phi_\infty$. The ensuing Kruskal manifold is invariant under the group of isometries $O(3,\mathbb{R})$ because the direct product $O(3,\mathbb{R}) \times O(3,\mathbb{R})$ operates transitively on the compact manifold of Keplerian orbits

$$\mathbb{S}^2 \times \mathbb{S}^2 \hookrightarrow \mathbb{R}^6 .$$

Dynamical symmetry breaking then provides the axisymmetric Kerr solution of Einstein's field equations mentioned above [13]. In view of the fact that the problem of determining the geodesic flow of the sub-Riemannian geometry of $G$ reduces to the isoperimetric problem in the plane at infinity of the compact Kähler manifold $\mathbb{CP}^2$, this is another justification of the projectivization method of the complexified coadjoint orbit picture of $\hat{G}$ in quantum information theory.

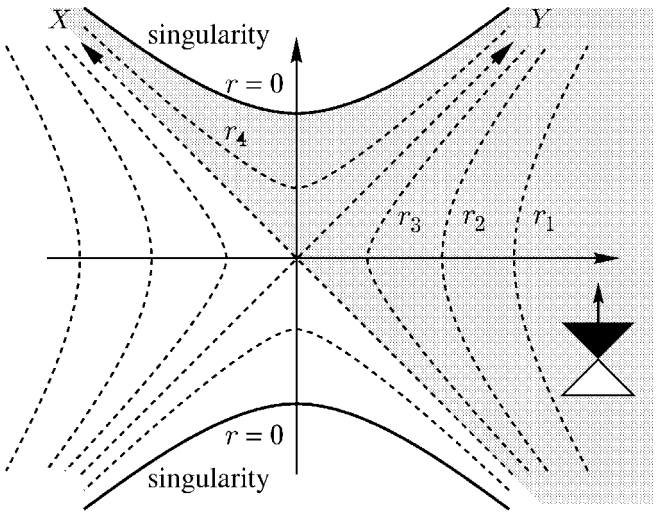


**Figure 11.** The Kruskal coordinatized two-fold covered Minkowskian spacetime manifold displaying radial null geodesics as straight line trajectories inclined at $45°$. The region in the Kruskal diagram covered by the Schwarzschild coordinate chart is shaded. The spatial metric is regular not only in the shaded area but in the entire area between the two branches of the hyperbola $r = 0$. This comprises two images of the exterior of the spherical singularity and two of its interior.

damping [67]. During the last 25 years of observations by Russel A. Hulse and Joseph H. Taylor (Nobel prize 1993) at the Arecibo Observatory Laboratory in Puerto Rico, a precession of the rotational axis of the radio pulsar PSR 1913+16 have not been observed so that the direction of the axis is perpendicular to the orbital plane. Because the pulse trains are *coherently* emitted [35], their phase and frequency coordinates can be registered by the symplectic affine spinorial substrates of quantum holography inside VLA radio interferometers. The simplest relativistic model of the binary system is in good accord with the data if both the "visible" radio pulsar and the silent companion cold star have approximately the Chandrasekhar limiting mass, 1.4 solar masses [41].

Outstanding successes of general relativity theory are the quantitative explanations of the precessions of the planetary perihelion as well as the motions of the periastron [21].

## 12. The Kaluza–Klein Model

One of the sad things about the hectic pace of modern science is that truly valuable discoveries and insights of earlier ages get completely forgotten. This is very true of projective geometry. The conjugate cyclic points $\{\bar{\mathrm{i}}, \mathrm{i}\}$ discovered by Jean Victor Poncelet (1788–1867) are common to all circles of the symplectic affine plane $\mathbb{R} \oplus \mathbb{R}$ having the compact Kähler manifold $\mathbb{CP}^2$ as the projectivization of its complexification. Because they give rise to the lightlike isotropic lines of any pencil of lines in the complex projective plane $\mathbb{CP}^2$, the zero-dimensional absolute projective quadric $\Phi^\circ_\infty$ is capable to serve as a phase reference. Its real trace can be observed in the pulse train diagrams of the 59-ms binary radio pulsar PSR 1913+16 [35] received by VLA radio interferometers. The compact unit sphere $\mathbb{S}^5 \hookrightarrow \mathbb{R}^6$ forms a circle bundle over $\mathbb{CP}^2$ and, by passing to the quotient, cuts down to the fundamental four-dimensional central Plücker quadric

$$\Psi \hookrightarrow \mathbb{RP}^5$$

of the Kaluza–Klein model of the Minkowskian spacetime manifold [13]. It allows to include Maxwell's laws of electrodynamics into a unified projective theory forming an interface of quantum theory and relativity theory, and to derive the Lorentz invariant Klein–Gordon equation. Conversely, the Einstein–Maxwell spinor [17] is invariant under the Lie group of rotational collineations of Lorentz transformations in $\mathbb{CP}^2$ which define via the Hopf fibration and the contragredient Hopf fibration the involution

$$\mathcal{O}_1 \leftrightarrow \mathcal{O}_{-1}$$

implemented by the assignment

$$\bar{\gamma} \quad \leftrightarrow \quad \underline{\gamma}.$$

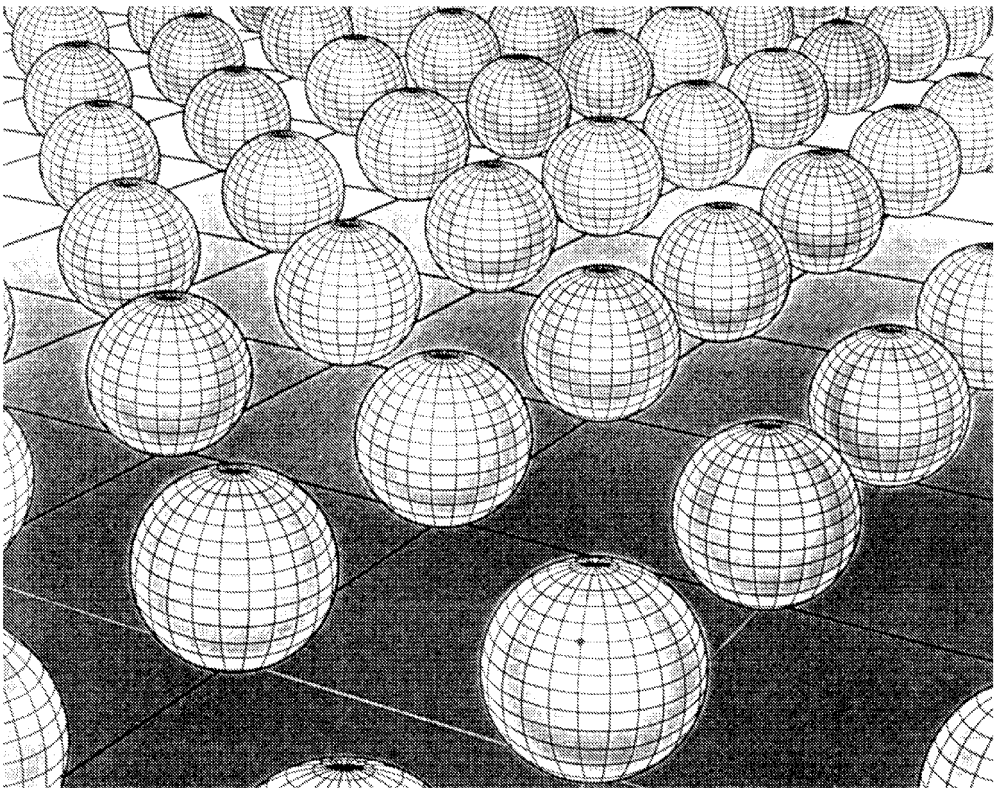

**Figure 13.** Visualization of the Klein–Kaluza model by spherical catenation. The one-dimensional central projective quadric $\Phi_\infty \hookrightarrow \mathbb{CP}^2$ is common to all the spheres of the periodic pencil of spheres. The plane represents the spacetime. One line of the plane represents the real axis of space, the perpendicular line represents the time axis.

The ensuing binary algorithm

$$\text{spin up} \quad \leftrightarrow \quad \text{spin down}$$

can be traced back to Gottfried Wilhelm Leibniz [22]. Bundles of quadrics allow to include general relativity via the Einstein–Maxwell equations for the coupled fields of electromagnetism and gravitation [42]. The transition in the Pauli sense from the real projective space $\mathbb{RP}^3$ to the four-dimensional Plücker quadric $\Psi$ of the space $\mathbb{RP}^5$ shows that the Lévy stochastic process of the spectral flow is *dual* to the associated phase coherent quantum field. Because the Heisenberg uncertainty principle has as its dual the channel noise, quantum holography can be considered as a line geometric duality theory which is based on the antisymmetric entanglement procedure of photonics and includes Bohr's complimentarity principle.

## 13. The Nine Projective Metric Geometries of the Plane

The four-dimensional central projective quadric $\Psi_\infty \hookrightarrow \mathbb{CP}^5$ as the absolute quadric of the Kaluza–Klein model allows to define the various projective metric geometries of the real plane. The following list provides a classification of the nine projective metric geometries to be realized by the real plane [42, 47].

| | curvature positive, no parallel lines, poles have no real tangent | curvature zero, one parallel line, poles have one tangent | curvature negative, several parallel lines, poles have two real tangents |
|---|---|---|---|
| polars $\cap\Phi_\infty = \emptyset$ | elliptic geometry | Euclidean geometry | hyperbolic geometry |
| polars $\cap\Phi_\infty$ = absolute pole | anti-Euclidean geometry | Galilean geometry | anti-Minkowskian geometry |
| polars $\cap\Phi_\infty$ = two points | anti-de Sitter world | Minkowskian world | de Sitter world |

In the plane $\mathbb{R} \oplus \mathbb{R}$ there are three Cayley–Klein geometries, the Euclidean, Galilean, and Minkowskian geometries with a parabolic measure of distance. The hyperbolic plane geometry can be realized by the Klein model of non-Euclidean plane. In the Minkowski plane geometry, all points have a common polar, the horizon connecting the conjugate cyclic points. The Milne cosmos carries the metric of the Minkowskian world, whereas the de Sitter cosmos can be equipped with the Friedman–Robertson–Walker metric to model the flat exponentially expanding cosmos, the positively curved contracting or expanding cosmos, or the negatively exploding cosmos [33]. Its singularity would imply that the universe had a beginning a finite time ago.

## 14. Visualizations of the de Sitter Worlds

Shortly after Einstein proposed the static model in 1917, de Sitter pointed out that the general relativistic field equations permitted the description of a second model. This was an expanding model of a spacetime manifold of constant curvature. Due to Hubble's discovery, the interest revived in it in the late 1920s. Recently it has regained interest in the context of the holographic principle and string theory [68].

The four-dimensional central projective quadric $\Psi$ in the complex projective space $\mathbb{CP}^5$ allows to visualize the geometries of the de Sitter cosmos as well as the anti-de Sitter cosmos. The Minkowski manifold, de Sitter manifold, and

anti-de Sitter manifold are all special cases of the Friedman–Robertson–Walker spaces. These spaces form a good approximation to the large scale geometry of spacetime manifold that can be observed [33].

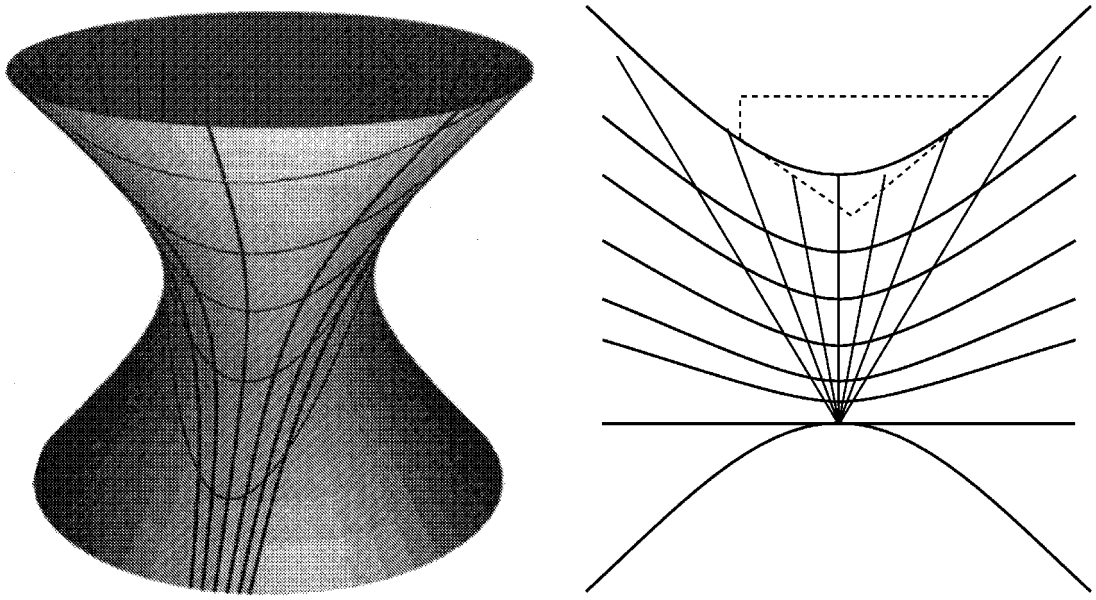

**Figure 14.** Exponentially expanding de Sitter cosmos of flat sections
The cosmological expansion is visualized by a ruled hyperboloid. Its projection onto a plane is also displayed. The absolute projective quadric is a hyperbola which meets the timelike lines.

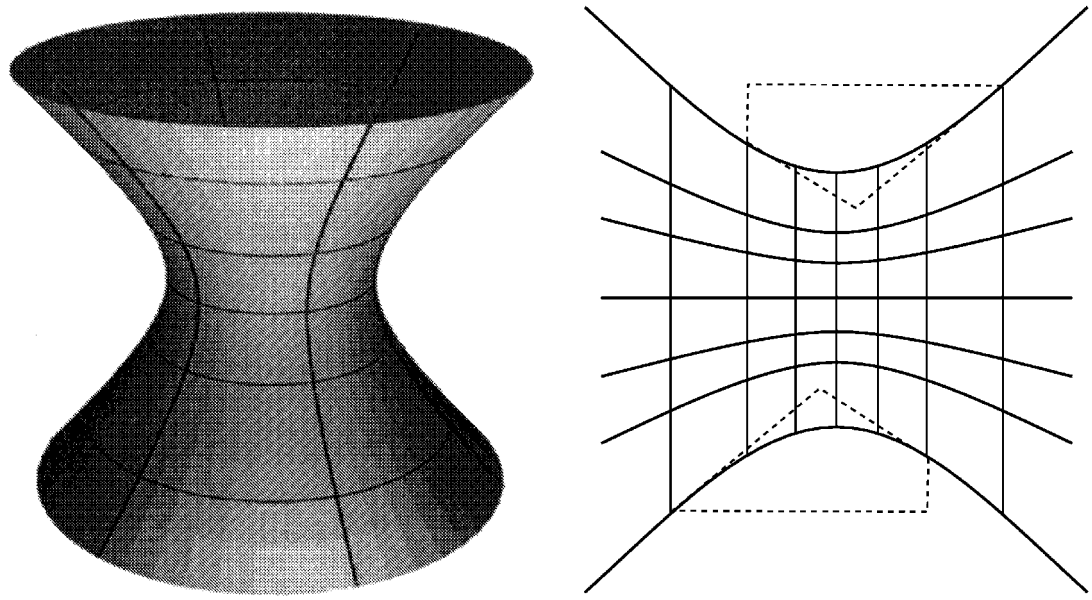

**Figure 15.** Contracting and expanding de Sitter cosmos with spatial sections of positive curvature. The pencil of timelike lines is carried by a point at infinity. In this case the curves of constant cosmological time are hyperbolas.

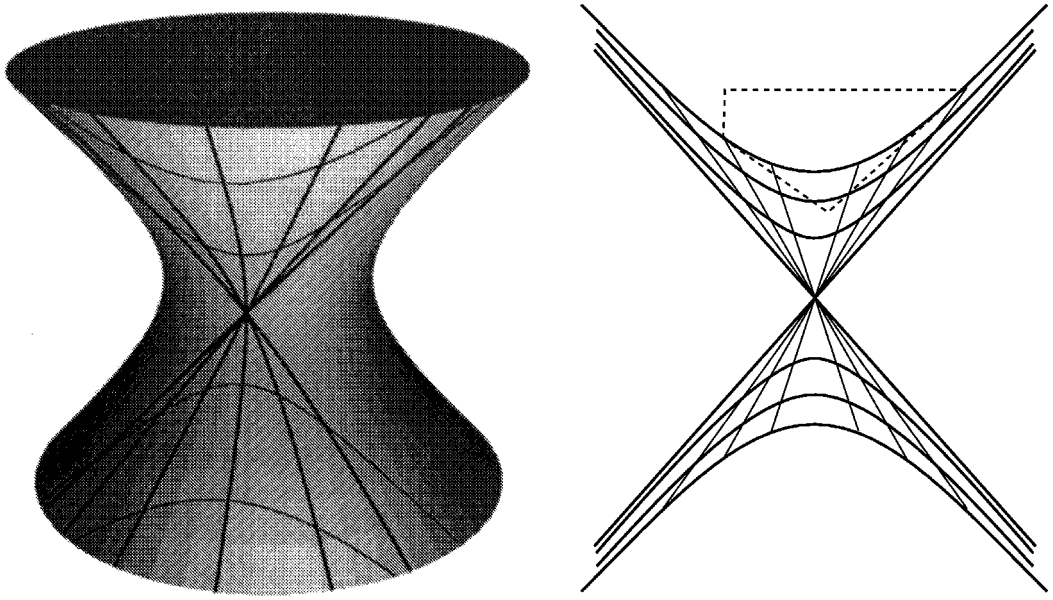

**Figure 16.** Expanding de Sitter cosmos with spatial sections of negative curvature. The projection of the hyperboloid onto a plane is also drawn. The pencil of timelike lines is carried by a point inside the world.

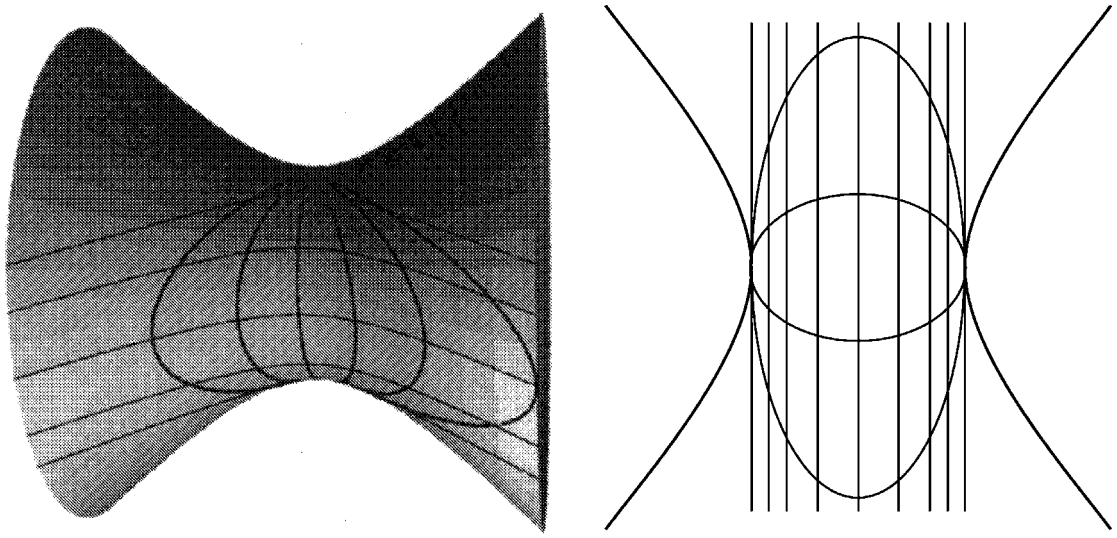

**Figure 17.** Expanding and contracting anti-de Sitter cosmos. The spatial sections have negative curvature. The absolute projective quadric forms a hyperbola which does not meet the timelike lines.

## References

[1] Abramson N., *Light-in-flight Recording: High-speed Holographic Motion Pictures of Ultrafast Phenomena*, Appl. Opt. **22** (1983) 215–232.

[2] Abramson N., *Light-in-flight Recording. 2: Compensation for the Limited Speed of the Light Used for Observation*, Appl. Opt. **23** (1984) 1481–1492.

[3] Abramson N., *Light-in-flight Recording. 3: Compensation for Optical Relativistic Effects*, Appl. Opt. **23** (1984) 4007–4014.
[4] Abramson N., *Light-in-flight Recording. 4: Visualizing Optical Relativistic Phenomena*, Appl. Opt. **24** (1985) 3323–3329.
[5] Abramson N. H. and Spears K. G., *Single Pulse Light-in-flight Recording by Holography*, Appl. Opt. **28** (1989) 1834–1841.
[6] Andrews M. R., Townsend C. G., Miesner H.-J., Durfee D. S., Kurn D. M. and Ketterle W., *Observation of Interference Between Two Bose Condensates* , Science **275** (1997) 637–641.
[7] Armitage J. V. and Rogers A., *Gauss Sums and Quantum Mechanics*, J. Phys. A: Math. Gen. **33** (2000) 5993–602.
[8] Bertoin J., *Lévy Processes*, Cambridge University Press, Cambridge, New York, Melbourne 1998.
[9] Binz E. and Schempp W., *Quantum Systems: From Macro Systems to Micro Systems — the Holographic Technique*, In: Cybernetics and Systems 2000, Vol. 1, (R. Trappl, Ed.), University of Vienna, Austrian Society for Cybernetic Studies, Vienna 2000, pp 123–128.
[10] Binz E. and Schempp W., *Vector Fields in Three-space, Natural Internal Degrees of Freedom, Signal Transmission and Quantization*, Result. Math. **37** (2000) 226–245.
[11] Binz E. and Schempp W., *Projective Geometry and Kepler's Libration Theory*, In: Proc. Int. Symposium on Quantum Theory and Symmetries, (H.-D. Doebner, J.-D. Hennig, W. Lücke and V. K. Dobrev, Eds), World Scientific, Singapore, New Jersey, London, Hong Kong 2000, pp 572–576.
[12] Binz E. and Schempp W., *The Art of Creating Magnetic Resonance Images*, In: Proc. Second Int. Workshop on Transforms and Filter Banks, (R. Creutzburg, J. Astola, Eds), Tampere International Center for Signal Processing, Tampere University of Technology, Tampere, Finland 2000, pp 571–589.
[13] Binz E. and Schempp W., *Entanglement, Parataxy, and Cosmology*, In: Proc. Leray Conference, Karlskrona 2000 (to appear).
[14] Binz E. and Schempp W., *Space-time Geometry and Quantum Information Transmission Detection*, (to appear).
[15] Binz E. and Schempp W., *The Landsberg–Schaar Identity and the Real Heisenberg Lie Group*, (to appear).
[16] Binz E. and Schempp W., *Lévy Process and Path Integral*, (to appear).
[17] Carmeli M., *Group Theory and General Relativity*, McGraw-Hill, New York, St. Louis, San Francisco 1977.
[18] Carrara W. S., Goodman R. S. and Majewski R. M., *Spotlight Synthetic Radar: Signal Processing Algorithms*, Artech House, Boston, London 1995.
[19] Cox D. A. and Katz S., *Mirror Symmetry and Algebraic Geometry*, Amer. Math. Soc., Providence, RI 1999.
[20] Curlander J. C. and McDonough R. N., *Synthetic Aperture Radar: Systems and Signal Processing*, J. Wiley & Sons, New York, Chichester, Brisbane 1991.
[21] Danzmann K. and Ruder H., *Gravitationswellen* , Phys. Bl. **49** (1993) 103–108.
[22] Deleuze G., *Le pli: Leibniz et le Baroque*, Les Éditions de Minuit, Paris 1988.

[23] Edelman R. R., Hesselink J. R. and Zlatkin M. B., *Clinical Magnetic Resonance Imaging*, 2nd edn, Vol. 1&2, W. B. Saunders, Philadelphia, London, Toronto 1996.

[24] Emery M., *Stochastic calculus in manifolds*. Springer-Verlag, Berlin, Heidelberg, New York 1989.

[25] Farre G. L., *The Energetic Structure of Observation*, Amer. Behav. Scient. **40** (1997) 717–728.

[26] Farre G. L., *Cosmic Evolution: Characteristics and Implications for the Philosophy of Nature*, Acta Polytech. Scand. **91** (1998) 3–11.

[27] Frieden B. R., *Applications to Optics and Wave Mechanics of the Criterion of Maximum Cramer–Rao Bound*, J. Mod. Opt. **35** (1988) 1297–1316.

[28] Gangolli R., *Isotropic Infinitely Divisible Measures on Symmetric Spaces*, Acta Math. **111** (1964) 213–246.

[29] González-Villanueva A., Guillaumín-España E., Núñez-Yépez H. N. and Salas-Brito A. L., *Scattering in a Coulomb Potential: A Velocity Space Point of View*, Rev. Mex. Fís. **44** (1998) 303–311.

[30] González-Villanueva A., Guillaumín-España E., Martínez-y-Romero R. P., Núñez-Yépez H. N. and Salas-Brito A. L., *From Circular Paths to Elliptic Orbits: A Geometric Approach to Kepler's Motion*, Eur. J. Phys. **19** (1998) 431–438.

[31] González-Villanueva A., Núñez-Yépez H. N. and Salas-Brito A. L., *In Velocity Space the Kepler Orbits Are Circular*, Eur. J. Phys. **17** (1996) 168–171.

[32] Grössing G., *Nonlocality and the Time-ordering of Events*, In: Cybernetics and Systems 2000, Vol. 1 (R. Trappl, Ed.) University of Vienna, Austrian Society for Cybernetic Studies, Vienna 2000, pp 185–188.

[33] Hawking S. W. and Ellis G. F. R., *The Large Scale Structure of Space–Time*, Cambridge University Press, Cambridge, New York, Melbourne 1973.

[34] Howe R., *A century of Lie theory*, In: Mathematics into the Twenty-first Century, Proc. AMS 1988 Centennial Symposium (F. E. Browder, Ed.) Amer. Math. Soc., Providence, Rhode Island 1992, pp 101–320.

[35] Hulse R. A. and Taylor J. H., *Discovery of a Pulsar in a Binary System*, The Astrophys. J. **195** (1975) L51–L53.

[36] Kunze R. A., *Positive Definite Operator-valued Kernels and Unitary Representations*, In: Functional Analysis, Proc. of a Conference held at the University of California, Irvine, (B. R. Gelbaum, Ed.), Thompson Book Company, Washington, DC 1967, pp 235–247.

[37] Kunze R. A., *On the Frobenius Reciprocity Theorem for Square-integrable Representations*. Pacific J. Math. **53** (1974) 465–471.

[38] Leith E. N., *Synthetic Aperture Radar*, In: Optical Data Processing, (D. Casasent, Ed.) Topics in Applied Physics, Vol. 23, Springer-Verlag, Berlin, Heidelberg, New York 1978, pp 89–117.

[39] Leith E. N., *Incoherent Optical Processing and Holography*, In: Optical Processing and Computing, (H. H. Arsenault, T. Szoplik and B. Macukow, Eds) Academic Press, Boston, San Diego, New York 1989, pp 421–440.

[40] Leith E. N., *Optical Processing of Synthetic Aperture Radar Data*, In: Photonic Aspects of Modern Radar, (H. Zmuda, E. N. Toughlian, Eds) Artech House, Boston, London 1994, pp 381–401.

[41] Lieb E. H., *The Stability of Matter: From Atoms to Stars*, Bull. (New Series) Amer. Math. Soc. **22** (1990) 1–49.

[42] Liebscher D.-E., *Einsteins Relativitätstheorie und die Geometrien der Ebene: Illustrationen zum Wechselspiel von Geometrie und Physik*, Verlag B.G. Teubner, Stuttgart, Leipzig 1999.

[43] Meyer P. A., *Éléments de Probabilités Quantiques*, Exposés I à V, Institut de Mathématiques, Université Louis Pasteur, Strasbourg 1984/85.

[44] Núñez-Yépez H. N., Guillaumín-España E., González-Villanueva A., Martínez-y-Romero R. P. and Salas-Brito A. L., *Newtonian Approach for the Kepler–Coulomb Problem from the Point of View of Velocity Space*, Rev. Mex. Fís. **44** (1998) 604–610.

[45] Panych L. P., *Theoretical Comparison of Fourier and Wavelet Encoding in Magnetic Resonance Imaging*, IEEE Trans. Med. Imag. **15** (1990) 141–153.

[46] Parthasarathy K. R. and Schmidt K., *Positive Definite Kernels, Continuous Tensor Products, and Central Limit Theorems of Probability Theory*, Lecture Notes in Math., Vol. 272, Springer-Verlag, Berlin, Heidelberg, New York 1972.

[47] Pickert G., *Analytische Geometrie*, 4. Auflage. Akademische Verlagsgesellschaft Geest & Portig, Leipzig 1961.

[48] Petry M. J., *Hegel on Newton, Colulomb and Bode: The background to The Orbits of the Planets*, In: Fessellos durch die Systeme, (W. Ch. Zimmerli, K. Stein und M. Gerten, Herausgeber) Verlag frommann-holzboog, Stuttgart-Bad Cannstatt 1997, pp 391–457.

[49] Rabin J. M., *Introduction to Quantum Field Theory for Mathematicians*, In: Geometry and Quantum Field Theory, (D. S. Freed, K. K. Uhlenbeck, Eds) IAS/Park City Mathematics Series, Vol. 1, Amer. Math. Soc., Providence, RI 1995, pp 183–270.

[50] Reed I. S., *A New Probabilistic Interpretation of $\psi\psi^\star$ Using Nonhomogeneous Poisson Statistics*, Digit. Sig. Proc. **1** (1991) 176–179.

[51] Reiser M. and Semmler W., Eds, *Magnetresonanztomographie*, 3. Auflage. Springer-Verlag, Berlin, Heidelberg, New York 2000.

[52] Salam A., *The Formalism of Lie Groups*, In: Theoretical Physics, International Atomic Agency, Vienna 1963, pp 173–196.

[53] de Sam Lazaro J. and Meyer P. A., *Méthodes de martingales et théorie des flots*, Z. Wahrscheinlichkeitstheorie verw. Geb. **18** (1971) 116–140.

[54] Schempp W., *Harmonic Analysis on the Heisenberg Nilpotent Lie Group, with Applications to Signal Theory*, Pitman Research Notes in Mathematics Series, Vol. 147, Longman Scientific & Technical, London 1986.

[55] Schempp W., *Quantum Holography and Neurocomputer Architectures*, In: Holography, (P. Greguss, T. H. Jeong, Eds), SPIE Institute of Advanced Optical Technologies, Vol. IS8, SPIE, Bellingham, WA 1991, pp 62–144.

[56] Schempp W. J., *Zu Keplers Conchoid-Konstruktion*, Result. Math. **32** (1997) 352–390.

[57] Schempp W. J., *Magnetic Resonance Imaging: Mathematical Foundations and Applications*, Wiley–Liss, New York, Chichester, Weinheim 1998.
[58] Schempp W., *Sub-Riemannian Geometry and Clinical Magnetic Resonance Tomography*, Math. Meth. Appl. Sci. **22** (1999) 867–922.
[59] Stark D. D. and Bradley Jr. W. G., Eds, *Magnetic Resonance Imaging*, Third Edition. Three Volumes, Mosby, St. Louis, Baltimore, Boston 1999.
[60] Stephenson B., *Kepler's Physical Astronomy*. Princeton University Press, Princeton, New Jersey 1994.
[61] Stiefel E. L. and Scheifele G., *Linear and Regular Celestial Mechanics*, Die Grundlehren der mathematischen Wissenschaften, Band 174. Springer-Verlag, Berlin, Heidelberg, New York 1971.
[62] Stumpff K., *Himmelsmechanik*, Band III. Deutscher Verlag der Wissenschaften, Berlin 1974.
[63] Sullivan R. J., *Microwave Radar: Imaging and Advanced Concepts* , Artech House, Boston, London 2000.
[64] Valdmanis J. A. and Abramson N. H., *Holographic Imaging Captures Light in Flight* In: Laser Focus World, February 1991, pp 111–117.
[65] Weil A., *Introduction à l'Étude des Variétés Kählériennes*, Actualités Scientifiques et Industrielles 1267, Hermann, Paris 1958.
[66] Weil A., *Sur certains groupes d'opérateurs unitaires*, Acta Math. **111** (1964) 143–211; Also in: *Collected Papers*, Vol. III (1964–1978), Springer-Verlag, New York, Heidelberg, Berlin 1980, pp 1–69.
[67] Weisberg J. M. and Taylor J. H., *Observations of Post-Newtonian Timing Effects in the Binary Pulsar PSR 1913+16*, Phys. Rev. Lett. **52** (1984) 1348–1350.
[68] Witten E., *Anti de Sitter Space and Holography*, Institute for Advanced Study Preprint, Princeton, New Jersey 1998.